DEVELOPMENTAL DYNAMICS 239:2172–2189, 2010

RESEARCH ARTICLE

# Ooplasmic Segregation in the Zebrafish Zygote and Early Embryo: Pattern of Ooplasmic Movements and Transport Pathways

**Ricardo Fuentes and Juan Fernández***

**Patterns of cytoplasmic movements and organization of transport pathways were examined in live or fixed zygotes and early zebrafish embryos using a variety of techniques. The zygote blastodisc grows by accumulation of ooplasm, transported to the animal pole from distinct sectors of ecto- and endoplasm at different speeds and developmental periods, using specific pathways or streamers. Slow transport (5 μm/min) occurs during the first interphase along short streamers, whereas fast transport (9.6–40 μm/min) takes place during the first cleavage division along axial and meridional streamers. Interconnections between streamers allow cargoes to change their speed and final destination. A similar sequence of events occurs during the following divisions. A complex network of microtubules and actin filaments in the endo- and ectoplasm appears to be involved in the transport of inclusions and mRNAs. Actin-dependent intermittent pulsations provoked high-speed back-and-forth movements of cytoplasm that may contribute to redistribution of organelles and maternal determinants. *Developmental Dynamics 239:2172–2189, 2010.***


**Key words:** ooplasmic segregation; early zebrafish development; cytoplasmic movements; zygote development; ooplasmic domains; zygote cytoskeleton; maternal mRNA localization and transportation

Accepted 24 May 2010

## INTRODUCTION

Ooplasmic domains are sectors of the egg cytoplasm that enclose organelles, cytoplasmic determinants, and cytoskeleton (Fernández and Olea, 1982, 1995; Bally-Cuif et al., 1998; Fernández et al., 1998, 2006). In many eggs, formation of these domains involves separation of yolk from the rest of the cytoplasmic components by a process called ooplasmic segregation. This process is essential to ensure normal embryonic development and occurs in the eggs of invertebrate and vertebrate organisms that exhibit mosaic or regulative development, respectively. In invertebrates, examples of such a segregation process are seen in the oligochaetes, which form conspicuous polar domains (Penners, 1922; Shimizu, 1982); leeches, which originate bizarre teloplasms (Whitman, 1878; Fernández and Olea, 1982); ascidians, which give rise to crescent-shaped domains (Conklin, 1905; Jeffery and Meier, 1983); nematodes and insects, which form germ plasm (Mahowald, 1962; Strome and Wood, 1983); as well as polychaetes and some molluscs, which form voluminous polar lobes (Wilson, 1904; Lillie, 1906). In vertebrates, an example is the formation of the embryonic disc, or blastodisc, that gives rise to most of the embryo in fishes, reptiles, and birds (Nelsen, 1953).

The zebrafish zygote is about 700 μm in diameter and consists of vitelloplasm, which contains yolk globules, and ooplasm. The ooplasm contains numerous organelles and forms three interconnected domains: a blastodisc at the top of the animal hemisphere, a layer of ectoplasm at the yolk cell periphery, and a network of endoplasmic lacunae in the yolk cell. Formation of these domains is initiated during oogenesis (Fernández et al., 2006; Lessman, 2009). The structure of this egg contrasts with that of other fishes such

Additional Supporting Information may be found in the online version of this article.

Laboratory of Developmental Cell Biology, Department of Biology, Faculty of Sciences, University of Chile, Santiago, Chile
Grant sponsor: Fondecyt; Grant number: Fondecyt 1030879 (2003–2006).
***Correspondence to: Juan Fernández, Laboratory of Developmental Cell Biology, Department of Biology, Faculty of Sciences, University of Chile, Casilla 653, Santiago, Chile. E-mail: jfernand@abello.dic.uchile.cl**

**DOI 10.1002/dvdy.22349**
Published online 21 June 2010 in Wiley InterScience (www.interscience.wiley.com).

as Medaka (reviewed by Hart and Fluck, 1995), in which the yolk forms a large body and endoplasm is not present.

The zebrafish zygote is a convenient cell model for the study of the mechanisms involved in several processes including fertilization, cytoplasmic movements driving ooplasmic segregation, localization and transit of maternal determinants, generation of calcium transients, and the establishment of cell polarity. Large amounts of ooplasm become segregated from yolk and translocate from one part of the zygote to another and finally accumulate in the blastodisc (Roosen-Runge, 1938; Katow, 1983; Leung et al., 2000). Concomitantly, numerous maternal mRNA transcripts travel across the ecto-or endoplasm and then accumulate in the blastodisc (Bally-Cuif et al., 1998; Howley and Ho, 2000; Hashimoto et al., 2004; Theusch et al., 2006). In this manner, the zygote becomes a polarized cell. The products of these transcripts are involved in the control of important events in early development such as egg activation (Mei et al., 2009), determination of the animal/vegetal axis (Marlow and Mullins, 2008), pronuclear fusion (Dekens et al., 2003), ooplasmic segregation (Dosch et al., 2004), cleavage (Jesuthasan and Strähle, 1996; Urven et al., 2006; Kishimoto et al., 2004), formation of the germ plasm (Knaut et al, 2000; Theusch et al., 2006; Kosaka et al., 2007; Bontems et al., 2009), and body axis formation (Mizuno et al., 1999; Ober and Schulte-Merker, 1999; Howley and Ho, 2000; reviewed by Bashirulla et al., 1998; Pelegri, 2003; Lindeman and Pelegri, 2009). Calcium transients are known to be generated during contraction of the actin ring and cleavage (Webb et al., 1997; Créton et al., 1998; Leung et al., 1998; Lee et al., 2006).

An advantage of live zygotes for microscopic observation is that they are translucent. Moreover, the differences in the refractive index of its components allows the tracking of yolk and ooplasmic inclusions (Iwamatzu, 1973; Leung et al., 2000). The visualization of ooplasmic movements is further improved by microinjection of a variety of probes such as labeled dextrans and beads (Jesuthasan and Strähle, 1996; Leung et al., 2000; Fernández et al., 2006) or carbon particles (Ivanenkov et al., 1990).

Ooplasmic segregation has been studied extensively in the zebrafish zygote since the pioneer work of Roosen-Runge (1938) and more recently by Leung et al. (1998, 2000) and Fernández et al. (2006). In the zebrafish and other fishes, the cytoskeleton has been considered to play an important role in ooplasmic segregation (reviewed by Hart and Fluck, 1995). Cortical microtubules are reported to be involved in the transport of foreign labeled particles and cytoplasmic determinants (Jesuthasan and Strähle, 1996; Gore and Sampath, 2002). Cortical actin filaments are known to assemble into a ring whose contraction is considered to be the motor driving ooplasmic segregation (Katow, 1983; Leung et al., 2000). Peripheral actin filaments are also claimed to participate in sperm penetration (Hart et al., 1992), cortical reaction (Becker and Hart, 1996), and transport of determinants involved in the formation of the germ plasm (Theusch et al., 2006). The presence of an internal or endoplasmic cytoskeleton in the zebrafish egg was suggested by Beams et al. (1985), who used scanning electron microscopy, and later demonstrated in oocytes and eggs by Fernández et al. (2006) using transmission electron microscopy.

In this report, we extend observations on the first steps of ooplasmic segregation in the stage V oocyte and egg (Fernández et al., 2006) to later events that take place in the zygote and early embryo, with emphasis on the structure of the cytoskeleton and the organization of pathways for the transport of cytoplasmic inclusions, fluorescent tracers, and maternal transcripts. The speed and direction of transport at different developmental stages were determined.

## RESULTS

### Ooplasmic Segregation in the Zebrafish Zygote Occurred in Three Stages That Correlated With Completion of Meiosis and Phases of the First Cell Cycle

We have subdivided development of the uncleaved embryo (total n=30) into three stages indicated here as stages 1a, 1b, and 1c. Stage 1a (completion of meiosis) extended from egg laying to the discharge of the second polar body. During this stage, the egg became turgid, released the second polar body, and the preblastodisc grew slightly to become the blastodisc (not shown; for details see Fernández et al., 2006). Stage 1b (first interphase) extended from discharge of the second polar body to the time at which the blastodisc adopted a biconvex shape and the contraction of the actin ring became evident at the margin of the blastodisc. At this stage, the egg flattened along the animal/vegetal axis and then recovered its spherical shape. The blastodisc underwent moderate growth (Fig. 1A–C). Stage 1c (first cleavage division) started with the onset of the actin ring contraction at the margin of the blastodisc and ended with the formation of the two first blastomeres. During early stage 1c, the long axial streamers were assembled and the blastodisc grew considerably due to the accumulation of ooplasm and yolk globules (Fig. 1D,E). During late stage 1c, the actin ring relaxed, the long axial streamers became less visible, and the blastodisc completed its first division (Fig. 1F). At 20–22°C, stage 1a was completed at 10–15 min, stage 1b at 45–60 min, and stage 1c at 60–75 min of development. At 25°C, stage 1a was completed at 5–10 min, stage 1b at 25–35 min, and stage 1c at 40–45 min of development. At 28°C, stage 1a was completed at about 5 min, stage 1b at 25–30 min, and stage 1c at 30–35 min. Accordingly, zygote development was completed at the following normalized time: 0.1–0.2, for stage 1a; 0.6–0.8, for stage 1b, and 0.8–1, for stage 1c.

To correlate staging of the one-cell embryo with periods of the first cell cycle, we studied DAPI-stained nuclear DNA in whole-mounted acid-fixed blastodiscs (total n=65). Results appear as insets to Figure 1. During stage 1a, the meiotic spindle, arrested in metaphase II, resumed development and in a few minutes discharged the second polar body (Fernández et al., 2006). Acid fixation often destroyed the polar body leaving DAPI-stained material attached to the blastodisc. This is considered to

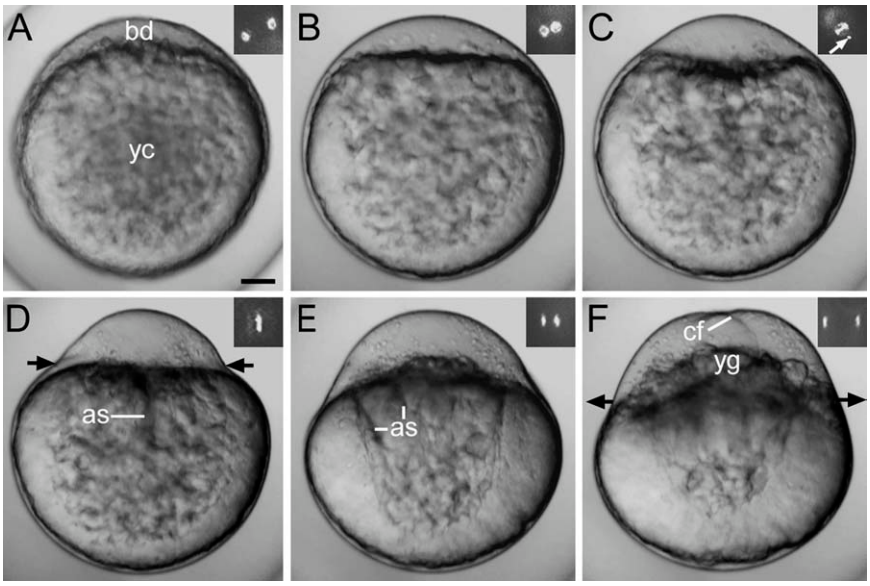


**Fig. 1.** Light microscope images showing the stages in the development of a live zygote (lateral view). **A:** Early stage 1b. **B:** Mid stage 1b. **C:** Late stage 1b. **D,E:** Early stage 1c. **F:** Late stage 1c. Insets show the organization of the DAPI-stained nuclear DNA. During early first interphase (A–C), the zygote nucleus formed close to the DAPI-stained spot (white arrow in C). Chromosomes are shown during the first cleavage division: metaphase (D), anaphase (E), and telophase (F). Inner-directed and outer-directed black arrows indicate contraction and relaxation of the actin ring, respectively. as, axial streamers; bd, blastodisc; cf, cleavage furrow; yc, yolk cell; yg, yolk globules. Development at 21°C. Scale bar = 70 μm.

be condensed chromatin that constitutes a reference point for the position of the animal pole. During stage 1b, pronuclei approached each other (inset in Fig. 1A,B) and their coalescence occurred close to the DAPI-stained spot leading to the formation of the zygote nucleus (inset in Fig. 1C). During stage 1c, the first mitosis was completed (inset in Fig. 1D–F). Our results confirmed and complemented observations of Streisinger et al. (1981) and Dekens et al. (2003).

Complex cytoplasmic movements, to be described in detail later, occurred during development of the zebrafish zygote. The direction and relative speed of these movements in different regions of the zygote and the contraction/relaxation cycle of the actin ring are summarized in Figure 2.

## Time-Lapse Video Imaging Showed That the Egg, Zygote, and Early Embryo Displayed Numerous Deformation Movements

Animated sequences prepared at short intervals of 10–30 sec (total n=35) revealed that development of the zebrafish egg was accompanied by numerous deformations. During stage 1a, the egg became turgid and released the second polar body. During stage 1b, the zygote exhibited an initial animal/vegetal flattening and exhibited intermittent deformations called pulsations. These were manifested by shortening and stretching of the embryo along its animal/vegetal axis. This phenomenon has not been described before. During stage 1c, there were further pulsations and a third type of deformation provoked by the contraction/relaxation of the actin ring. This was a cyclic phenomenon that also took place at the margin of the cleaving blastoderm and in water-activated zebrafish eggs (Kane and Kimmel, 1993). Pulsations also continued during early cleavage and their number and extension varied from zygote to zygote. At temperatures of 22–25°C, high-frequency pulsations extended from less than a minute to 2–3 min (see Supp. Video S1, which is available online), whereas low-frequency pulsations extended for several minutes. We have counted up to 19 episodes of pulsation in a zygote. The extent and number of pulsations increased with the age of the embryo. High-frequency pulsations, similar to those described above, also occurred at higher temperatures (25–28°C).

Discharge of the second polar body, pulsations, contraction/relaxation of the actin ring, ooplasmic segregation, blastodisc growth, and pseudo cleavage also took place in the unfertilized egg (see also Kane and Kimmel, 1993), indicating that these processes do not depend on the formation of the zygote nucleus and the establishment of a normal cell cycle.

## Reorganization of the Endoplasm Studied in Acid-Fixed Embryos

The blastodisc grows mostly at the expense of endoplasm transported pole-ward from the yolk cell. Therefore, changes in the organization of the endoplasm during blastodisc enlargement provide important information on how this process progresses during early development. To this end, numerous eggs (n=10), zygotes (n=50), and early embryos (n=30) were examined after acid fixation at different time intervals. This technique allowed detailed visualization of the endoplasm, particularly after application of the inverse contrast facility of Metamorph software. Use of low concentrations of acetic or isobutyric acid (see Experimental Procedures section) minimized retraction of the lacunae from the vegetal ectoplasm. In the freshly laid egg, the interconnected endoplasmic lacunae appeared scattered throughout the entire yolk cell. Fine channels were seen linking the lacunae with one another, with the peripheral ectoplasm and the animally located blastodisc. Reorganization of the endoplasm advanced at different rates in different activated eggs and exhibited four main features: (1) fusion of the animal-most endoplasmic lacunae with the blastodisc to form short streamers (Fig. 3A), (2) coalescence and remodeling of animal and some equatorially located lacunae to form sinuous channels or long axial streamers connected to the blastodisc (Fig. 3B), (3) coalescence and remodeling of lacunae lying under the peripheral palisade of yolk globules to form the long meridional streamers, also

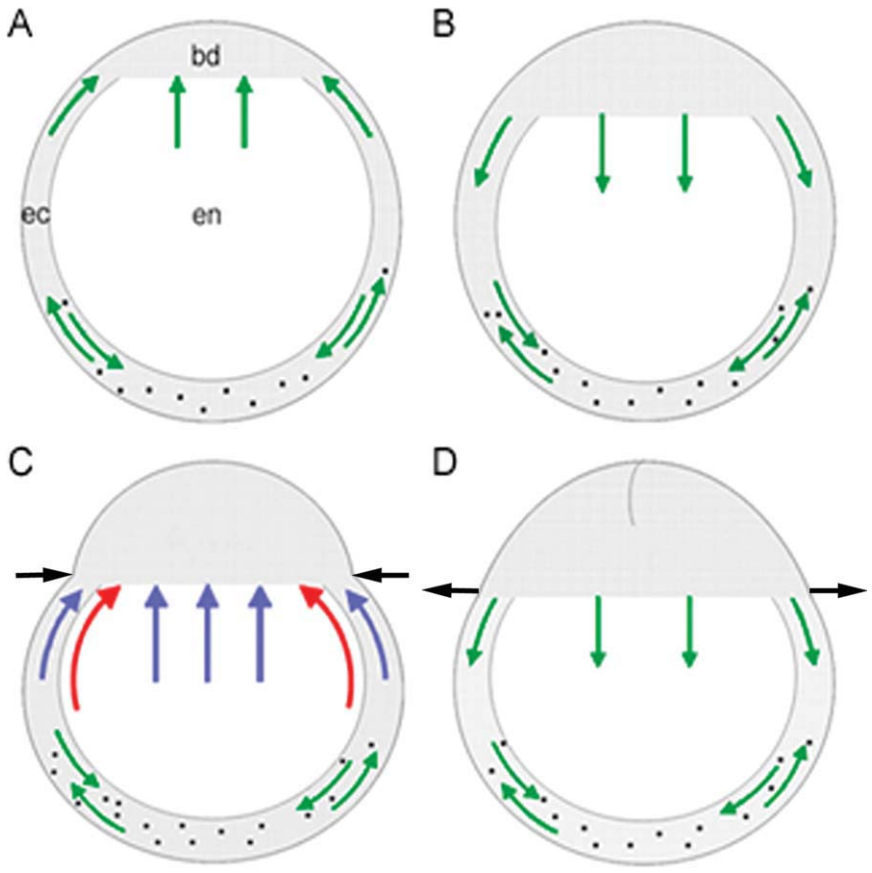


**Fig. 2.** Diagram that illustrates the contraction/relaxation cycle (inner-directed and outer-directed black arrows, respectively) of the actin ring and the movement of cytoplasmic inclusions, toward or away from the blastodisc (bd), across the ectoplasm (ec) and endoplasm (en) of early/mid stage 1b (**A**), late stage 1b (**B**), early stage 1c (**C**), and late stage 1c (**D**) zygotes. Lateral views. Small green arrows indicate the direction of low-speed movements, along the ectoplasm or short streamers in the endoplasm; mid-size blue arrows indicate the direction of high-speed movements, along the ectoplasm or long axial streamers in the endoplasm; and large red arrows indicate the direction of ultra-high-speed movements, along meridional streamers in the peripheral endoplasm. Black dots indicate the presence of numerous stationary inclusions.

connected to the blastodisc (Fig. 3C). Both types of long streamers formed by the time the animal actin ring started contracting and (4) pole-ward displacement of the vegetal endoplasmic lacunae that coalesced and joined the axial streamers. In some eggs, pole-ward displacement of the vegetal lacunae was initiated soon after egg activation, but usually this process started during the first cleavage division. In a few zygotes (less than 1%), vegetal lacunae fused at the center of the yolk cell to form a fenestrated body. In spite of differences in the rate of animal-ward movement of the vegetal lacunae, the pattern of endoplasm reorganization was similar in different embryos. Emptying of lacunae into the blastodisc was completed after several cleavage divisions.

## Reorganization of the Endoplasm Studied in Live Non-Injected Embryos

To complement observations on acid fixed cells, animations of live zygotes and embryos, up to the fourth or fifth cleavage division, were prepared using the inverted contrast facility of Metamorph (total n=18). Under these conditions, lacunae and streamers were visualized with less resolution than in acid-fixed cells, but it allowed us to follow the reorganization of the endoplasm in the living cell. The results confirmed observation on acid-fixed cells and also provided additional information. First, during the first interphase, vegetal lacunae suffered local displacements, remaining in similar regions of the vegetal yolk cell. At the same time, the animal-most lacunae were seen joining the blastodisc and forming short streamers (Fig. 3D). Second, the long axial and meridional streamers were formed at the beginning of each cell division, in synchrony with the contraction of the actin ring, and moved endoplasm toward the animal pole (see Supp. Videos S2, S3). Vegetal lacunae emptied their endoplasm into the axial streamers in an ordered sequence, starting with the equatorially located lacunae (Fig. 3E) and ending with the central most vegetally located ones (Fig. 3F). Third, during relaxation of the actin ring, streamers were less visible (Fig. 3G) and endoplasmic lacunae that remained in the yolk cell moved toward the animal pole. As expected, during cleavage divisions endoplasmic lacunae gradually diminished in number and streamers became thinner (Fig. 3H,I). Beyond the fourth or fifth cleavage division, many embryos lacked visible endoplasmic lacunae.

## Organization of the Cytoskeleton in the Endoplasmic Lacunae and Streamers

Immunofluorescence staining of the cytoskeleton was performed in whole-mount or frozen-sectioned zygotes and examined by confocal (n=16), fluorescence (n=27), or regular video light microscopy (n=5). Low-magnification confocal images of the yolk cell, selected from individual slices of a stack of images, showed that the endoplasmic lacunae include a cytoskeleton of actin filaments (Fig. 4A) and microtubules (Fig. 4B). Rotation of the stack of images revealed that the endoplasmic lacunae were irregularly shaped cytoskeleton-rich interconnected narrow spaces between the yolk globules. Higher magnification confocal images, taken from similar stacks, revealed two important features of the lacunae. First, that microtubules and actin filaments assembled into thin bundles that form a tight network and, second, that the network was three-dimensional because it occupied the entire volume of the lacuna (Fig. 4C–E). Large bundles of microtubules or microfilaments, such as those

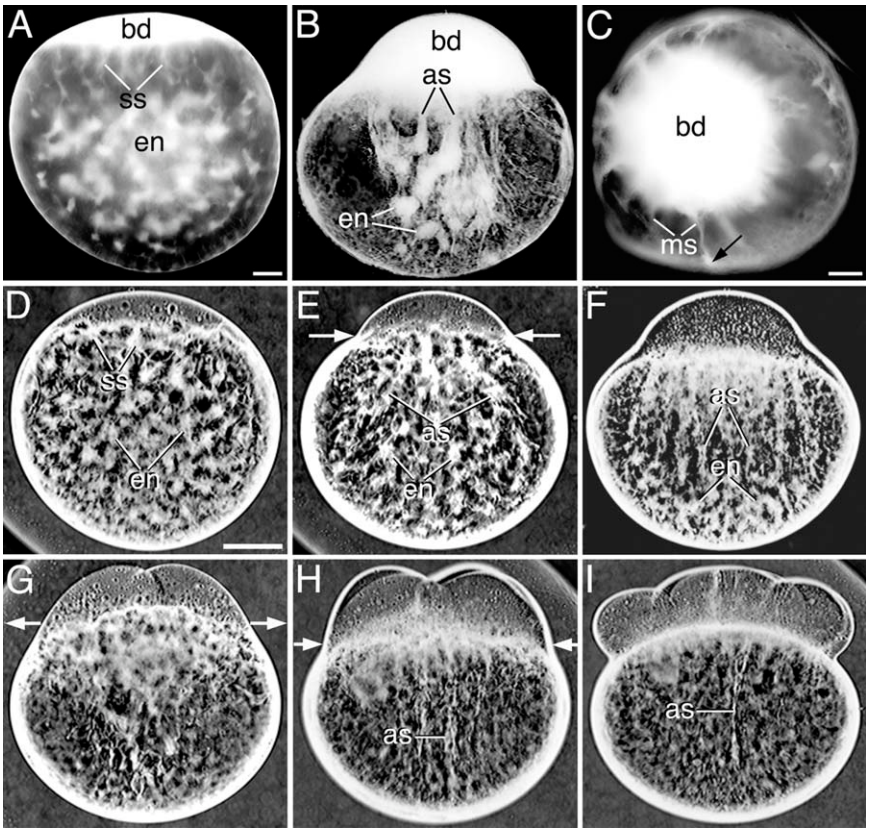


**Fig. 3.** Light microscope images showing the reorganization of the endoplasm (en) in inverted contrast acid-fixed (A–C) and live whole-mounted zygotes and embryos (D–I) during the first 3 cell cycles. **A:** Early first interphase, lateral view. **B:** Early first cleavage division, lateral view. **C:** Early first cleavage division, animal pole view. The arrow in C points to the peripheral localization of a meridional streamer (ms). Lateral views of: **D:** Early first interphase. **E,F:** Early first cleavage division. **G:** Two-cell embryo. **H:** Four-cell embryo. **I:** Eight-cell embryo. as, long axial streamers; bd, blastodisc; ss, short streamers. Scale bars = 80 μm (A–C), 160 μm (D–I).

formed in the vegetal pole of early zygotes (Jesuthasan and Strähle, 1996), were not visualized across the endoplasm.

Fluorescence images show that in some lacunae, cytoskeletal bundles appear disorganized (Fig. 4F), dispersed (Fig. 4G), or forming a loosely arranged network (Fig. 4K–M). These results indicate that the cytoskeleton in the lacunae exhibit different types of organization that may be related to the functional state of the cytoskeleton or its preservation. Differences in the structure of the cytoskeleton may explain the presence of different types of lacunae in sectioned early unfertilized eggs (Fernández et al., 2006). Mid-magnification confocal deconvolved images of double-immunostained lacunae selected from a stack of images showed that actin filaments and microtubules appeared to co-localize (compare Fig. 4H and I). However, analysis of merge images (Fig. 4J) indicated that actin filaments and microtubules formed separated or mixed bundles. This was confirmed by high-magnification confocal deconvolved images of double-immunostained lacunae selected from a similar stack of optical slices, revealing that in merged images microtubules and actin filaments formed separated bundles 0.5–1.5 μm in thickness. In several places, however, cytoskeletal bundles appeared yellow to orange, suggesting that in this case microtubules and actin filaments were intermixed and hence co-localized within the bundle. The three type of bundles appeared intercalated within the cytoskeletal network (Fig. 4K–M). In conclusion, the available evidence suggests that the cytoskeleton network in the endoplasmic lacunae consists of both "pure" and intermixed bundles of microtubules and actin filaments. The peripheral meshwork of microtubules and actin filaments observed under the fluorescence microscope (Fig. 4N) is similar to that seen in the internal cytoskeleton (lacunae and streamers) and resembles that described in the cortex of zebrafish (Hart et al., 1992; Becker and Hart, 1996, 1999) and other teleost eggs (reviewed by Hart and Fluck, 1995). Neither microtubules nor actin filaments were detected in controls incubated only with the second antibody (Fig. 4O). We have on occasion detected large ectoplasmic bundles of microtubules in the vegetal ectoplasm (Fig. 4P) of early stage-1b zygotes that resemble those described in the same region by Jesuthasan and Strähle (1996). As shown in Figure 4Q, microtubules can also be seen in endoplasmic lacunae of fragmented zygotes immunostained by a routine procedure such as that utilized by Jesuthasan and Strähle (1996). Filamentous structures, suggesting cytoskeletal components, were undetected in fluorescent-dextran microinjected control zygotes (Fig. 4R).

## Slow Movement of Endoplasm and Ectoplasm During the First Interphase (Stage 1b)

### *Animal-Ward Movement of Endogenous and Exogenous Markers Along the Ecto and Endoplasm During Early and Mid First Interphase (Early and Mid Stage 1b).*

The dynamic behavior of ectoplasmic and endoplasmic inclusions (n=25), microinjected-labeled beads (n=15), and dextran (n=7) was studied in animations prepared at 10–30-sec intervals. Ooplasmic inclusions were rounded or oval-shaped bodies that had a low-density interior and a refractive periphery. The smallest (1–3 μm in diameter) may correspond to vacuoles, whereas the largest (up to 20 μm in diameter) may be yolk globules. Vacuoles and small yolk globules are present in the egg ooplasm (Fernández et al., 2006). In the animal-most ecto- and endoplasm, inclusions and fluorescent beads preferentially moved toward the animal pole and

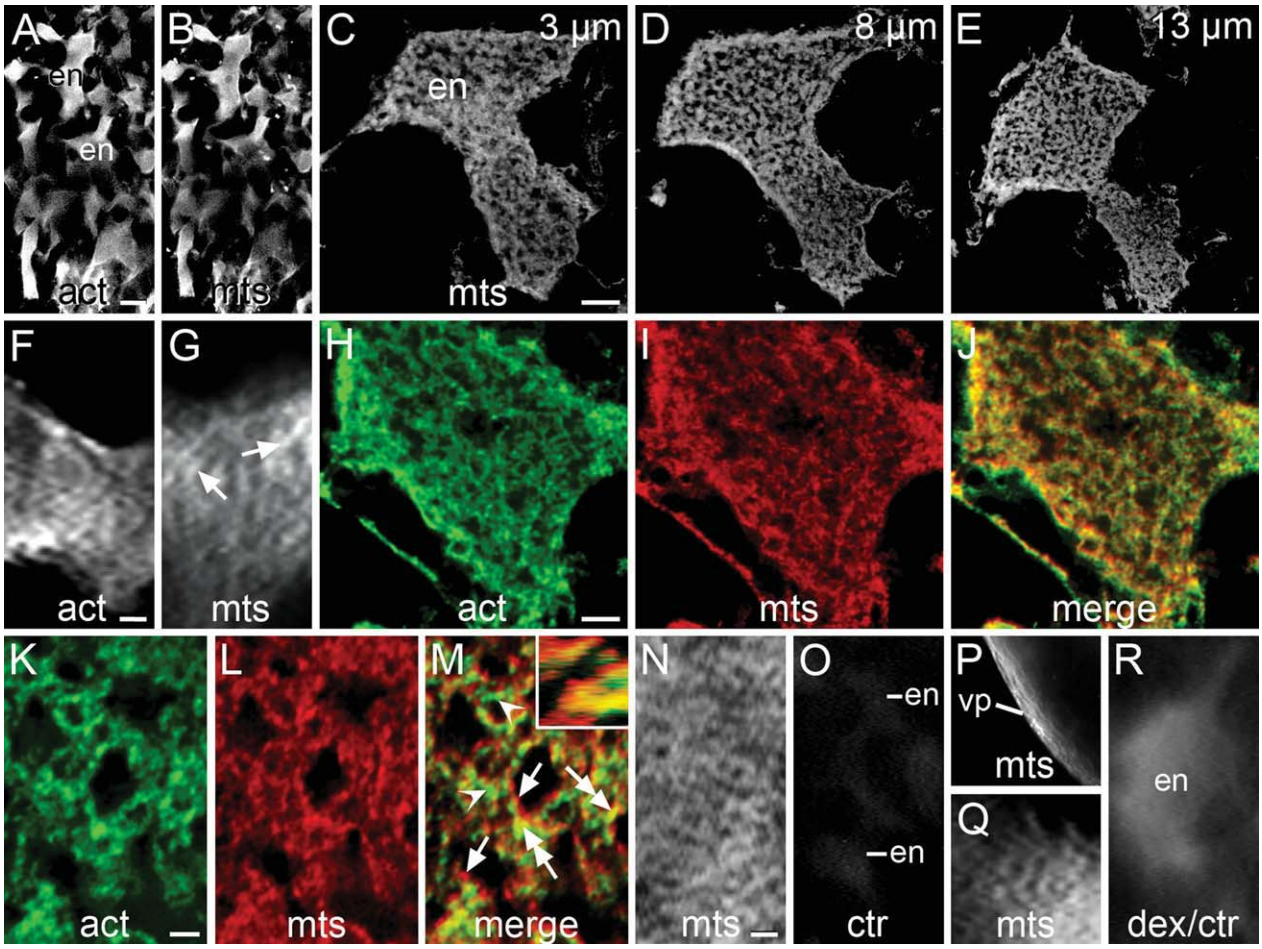


**Fig. 4.** Organization of the cytoskeleton in whole-mounted early stage 1b zygotes immunostained for actin filaments (act) and/or microtubules (mts) viewed under the confocal (A–E, H–J, K–M) or fluorescent (F, G, N–R) microscope. **A,B:** Confocal low-magnification images of the endoplasmic lacunae (en) stained for actin filaments (act) and microtubules (mts). **C–E:** Deconvolved confocal images selected from a z-stack containing 15× 1 μm-thick optical sections across an endoplasmic lacuna stained for microtubules. The position of the section within the stack is indicated. **F:** Lacuna showing a disorganized network of actin filaments. **G:** Lacuna showing dispersed bundles of microtubules (arrows). **H–J:** Deconvolved confocal intermediate magnification images of double immunostained lacuna selected from a z-stack of 15× 1-μm-thick optical sections. Shown is the network of actin filaments (H) and microtubule bundles (I) and the merged image of them (J). In the latter image, cytoskeletal bundles are seen as green dots (actin), red dots (microtubules), or yellow to orange dots (mixed actin and microtubules). **K–M:** Deconvolved confocal high-magnification images of double-stained lacuna, taken from a z-stack of 18× 1-μm-thick optical sections. It shows a loosely arranged cytoskeletal network built upon intercalated bundles of actin filaments (arrowheads), bundles of microtubules (arrows), and mixed bundles of actin filaments and microtubules (double-headed arrows). This condition is also illustrated in the optical cut along the X axis shown in the inset of M. **N:** Network of microtubules in the ectoplasm. **O:** Control incubated in the second antibody only. Lacunae are barely seen after a 20-second exposure. **P:** Bundles of oriented microtubules in the ectoplasm of the vegetal pole (vp). **Q:** Weakly stained microtubules in a lacuna immunostained according to Jesuthasan and Strähle (1996). **R:** Control showing an endoplasmic lacuna filled with rhodamine-labeled dextran. Notice the absence of fibrilar profiles. Scale bars = 10 μm (A–E), 6 μm (F), 5.5 μm (G), 5 μm (H–J), 2 μm (K–M), 5.6 μm (N), 10.5 μm (O), 15 μm (P), 4 μm (Q), 2 μm (R).

frequently entered the blastodisc (Fig. 5A,B; see Supp. Video S4). Fluorescent beads were seen moving directly from animal endoplasmic lacunae into the blastodisc (Fig. 5C) or to the neighboring ectoplasm and from here to the blastodisc (Figs. 5D–F; see Supp. Video S5). Movement of inclusions or fluorescent beads was irregular with zigzagged trajectories, back-and-forth displacements, and pauses. Intermittent or saltatory motions were also observed (Fig. 5G–H). Inclusions moved at an average low speed of 5.0 μm/min and fluorescent beads at 9.1 μm/min. Statistical analysis of these movements is shown in Figure 5I and J. In the rest of the endoplasm, objects were seen moving slowly and in several directions. Something similar occurred across the vegetal ectoplasm. Fluorescent dextran (not shown) confirmed observations described above in that endoplasm in the animal-most lacunae moved slowly and poured their content into the blastodisc. Endoplasm in the remaining lacunae showed local displacements or remained more or less in place. Unfertilized eggs behave similarly.

### *Vegetal-Ward Movement of Endogenous and Exogenous Markers Along the Ecto- and Endoplasm During Late First Interphase (Late Stage 1b) (n=14).*

During this stage, inclusions and fluorescent markers were seen moving slowly (average speed 5.0 μm/min for

**TABLE 1. Changes in the Volume of the Blastodisc and Yolk Sphere, Expressed in Nanoliters, During the First Interphase (Stage 1b)[a]**

| | Blastodisc | | | Yolk cell | | |
|---|---|---|---|---|---|---|
| Zygote | $_iV$ (nl) | $_fV$ (nl) | % of volume increase | $_iV$ (nl) | $_fV$ (nl) | % of volume decrease |
| 1 | 6.4 | 13.6 | 110.6 | 138.9 | 116.1 | 16.5 |
| 2 | 10.7 | 17.7 | 66.4 | 122.7 | 120.6 | 1.7 |
| 3 | 6.9 | 16.8 | 143.3 | 145.2 | 124.8 | 14.1 |
| 4 | 7.6 | 10.0 | 31.6 | 141.2 | 133.4 | 5.5 |
| 5 | 7.5 | 13.2 | 76.1 | 139.5 | 130.6 | 6.3 |
| 6 | 6.2 | 8.8 | 41.5 | 142.4 | 128.5 | 9.7 |
| 7 | 5.6 | 11.6 | 108.3 | 134.5 | 123.2 | 8.4 |
| 8 | 8.2 | 9.9 | 20.4 | 136.7 | 126.4 | 7.6 |
| 9 | 8.1 | 12.2 | 50.9 | 130.6 | 128.5 | 1.6 |
| 10 | 8.0 | 9.2 | 15.2 | 136.1 | 126.9 | 6.8 |
| **% of average volume change** | | | **+63.6** | | | **−8.0** |

[a]The initial ($_iV$) and final ($_fV$) volume of the blastodiscs and yolk spheres were determined from measurements performed on imaged live zygotes. Increases in the final volume of the blastodisc and decreases in that of the yolk sphere were variable but the values, calculated by the one-way ANOVA test, appeared significant ($P = 0.0003085$, for the blastodisc and $P = 0.0005245$, for the yolk cell), indicating that the slow flow of ecto- and endoplasm contributed to the blastodisc growth. For more details, see Experimental Procedures section.

the inclusions and 9.1 μm/min for the fluorescent beads) toward the vegetal pole. This movement included objects in the blastodisc and adjacent regions of the ectoplasm and it was accompanied by a change in the blastodisc to form a biconvex-shaped structure. This phenomenon was produced by vegetal-ward displacement of the blastodisc floor, presumably triggered by contraction of the endoplasmic actin cytoskeleton (Fig. 1C).

### *Blastodisc Growth During the First Interphase (n=10).*

Table 1 shows that during the first interphase there is an increase in the volume of the blastodisc and a decrease in the volume of the yolk sphere, confirming that the slow animal-ward flow of ecto- and endoplasm contributed to the blastodisc growth. There were differences between the initial and final volume, as well as in the percentage of volume growth of the individual

**Fig. 5.** Lateral view of whole-mounted mid stage 1b zygotes and graphs illustrating the slow movement of endoplasm during the first interphase. **A,B:** Still frames from a light microscope time-lapse video animation, taken at 10-sec intervals, showing that enlargement of the blastodisc (bd) is accompanied by the slow incorporation of endoplasmic inclusions (marked by yellow dots). Time elapsed between the images is indicated. Development at 24°C. **C:** Still frame from a time-lapse video animation taken every 10 sec showing the slow transport (arrow) of fluorescent beads (fb) from two endoplasmic lacunae (en) into the blastodisc (bd) by short streamers (ss). The probe was microinjected in the medial region of the yolk cell close to the blastodisc. **D–F:** Still frames from a time-lapse video animation taken at 30-sec intervals, showing the slow transport of fluorescent beads from the endoplasm to the ectoplasm (ec) and from here to the blastodisc (arrows). In this case, the probe was microinjected laterally close to the ectoplasm. Development at 20°C. Time in minutes between the images is indicated. **G, H:** Mid stage 1b zygote showing the irregular animal-ward trajectory of inclusions across the endoplasm (G) and ectoplasm (H). The consecutive positions of the inclusion, at 30-sec intervals, are marked with a red circle and the entire trajectory with a straight line linking the circles. Arrowheads indicate the direction of movement. The entire trajectory of the inclusion was saved in the first image of the respective stack. Development at 24–25°C. yc, yolk cell. **I,J:** Graphs showing the distribution of speeds of slow-moving ooplasmic inclusions (I) and fluorescent beads (J) in whole-mounted stage-1b zygotes. The black line is a Gaussian curve fitted to the experimental data. The central value and standard deviations are 5.0 ± 0.4 μm/min, for the inclusions, and 9.1 ± 0.9 μm/min, for the fluorescent beads. Scale bars = 55 μm (A, B), 40 μm (C–F), 8 μm (G, H).

**Fig. 6.** Lateral view of whole-mounted zygotes and graphs illustrating the fast movement of endoplasm during the first cleavage division. **A,B:** Still frames from a time-lapse video animation of light microscope images, taken at 10-sec intervals, of an early stage 1c zygote. Contraction of the actin ring has been initiated with fast movement of endoplasm and yolk globules (arrowhead) into the blastodisc (bd). Time in minutes between the images is indicated. **C–E:** Still frames from a time-lapse video animation, taken at 2-min intervals, of a zygote microinjected at the center of the yolk cell with rhodamine-labeled beads at early stage 1b. **C:** Mid stage 1b zygote showing fluorescent beads (fb) remaining at the site of injection. **D:** Early stage 1c zygote showing the animal-ward movement of the fluorescent beads along the axial streamers (as). **E:** Two-cell embryo with a relaxed actin ring and beads accumulated at the blastoderm/yolk cell boundary zone. Time elapsed between the images is indicated. Development at 20°C. **F,G:** Still frames from a time-lapse video animation taken at 10-sec intervals showing the transient connection (arrows) between a meridional streamer (ms) and the vegetal ectoplasm (ec). Time elapsed between the images is indicated. Development at 24°C. **H,I:** Fast straight movement of an ooplasmic inclusion along an axial streamer (H) and of a fluorescent bead along a meridional streamer (I). The position of the inclusion or bead was marked at each time interval (10 sec) with a red circle and the whole trajectory with a straight line linking the circles. These were saved in the first image of each stack. Arrowheads indicate the direction of movement. Development at 24–25°C. **J,K:** Graphs showing the distribution of speeds of fast-moving ooplasmic inclusions and fluorescent beads in whole-mounted early stage 1c zygotes. The black lines are the sum of two Gaussian curves fitted to the experimental data. The central values of the curves are: 9.6 ± 3.3 μm/min and 40.0 ± 2.8 μm/min, for the fast and ultra-fast movement of inclusions (J), and 39 ± 1.3 μm/min and 73.0 ± 3.9 μm/min, for the fast and ultra-fast movement of fluorescent beads (K). High speeds were less represented in the graphs (compare with the slow speeds in the graphs of Fig. 5) because fast-moving objects were difficult to track. oi, ooplasmic inclusion. Scale bars = 120 μm (A,B), 60 μm (C–E), 15 μm (F–I).

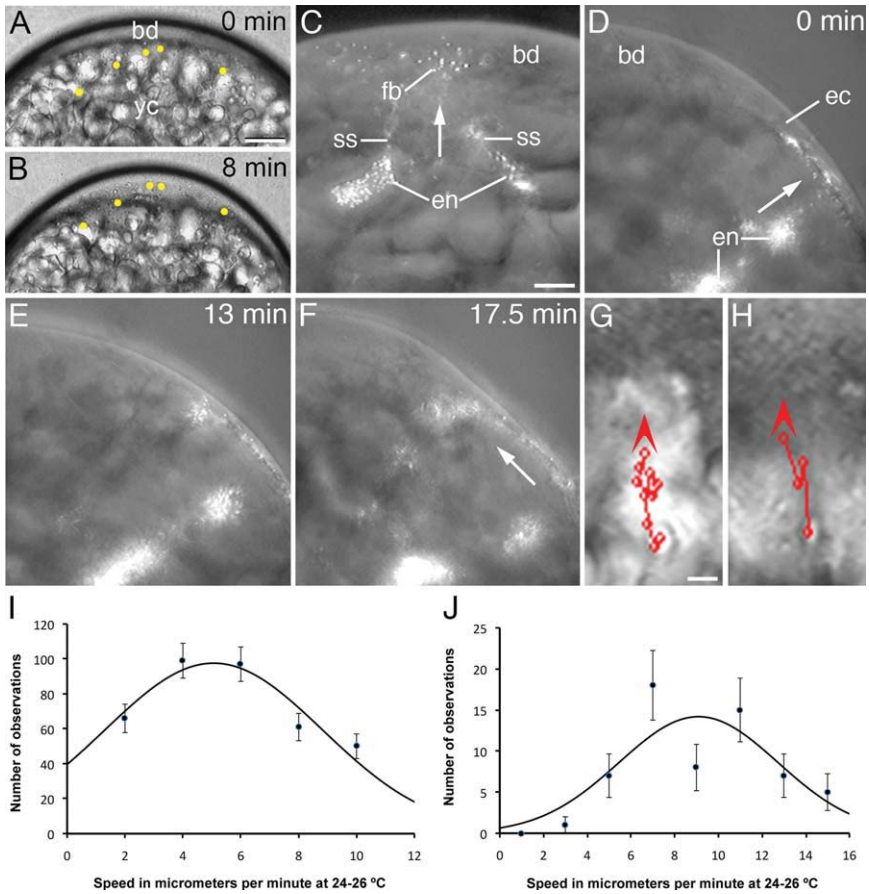


Fig. 5.

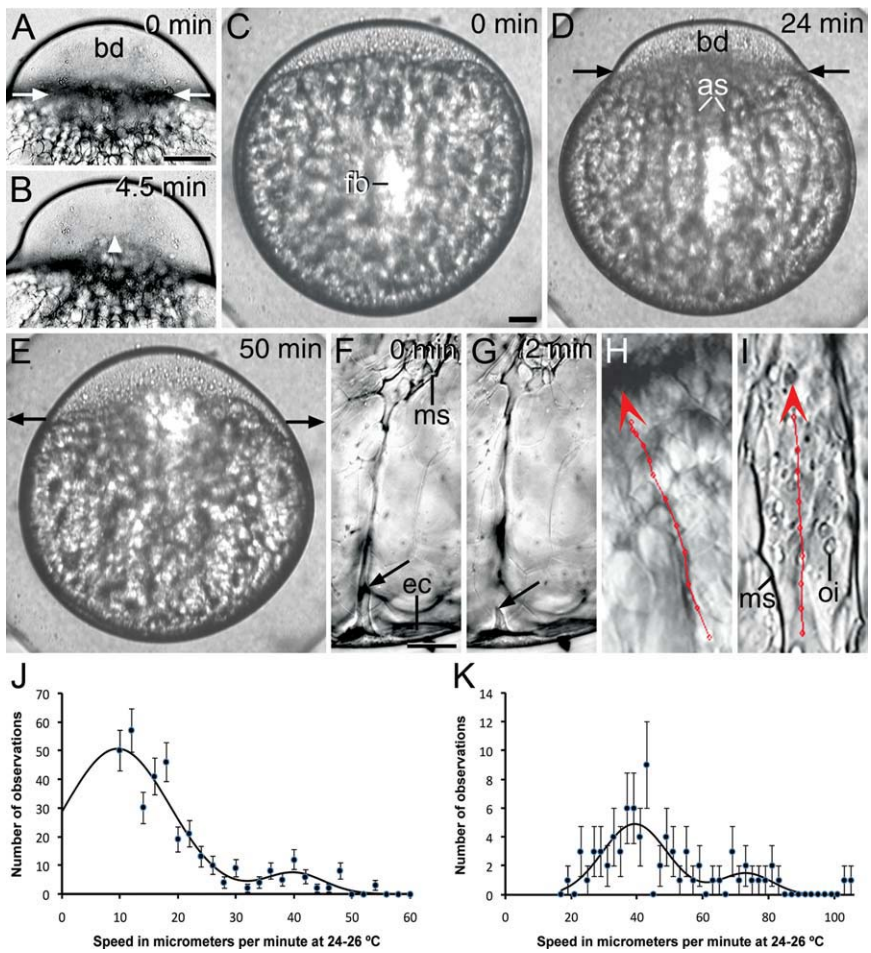


Fig. 6.

blastodiscs (average 63.6%). Similar changes occurred in the initial and final volume and in the percentage of volume decrease of the individual yolk cells (average 8%). These differences may be due to idiosyncratic variations in the speed at which zygotes developed and ooplasm moved to the blastodisc. In addition, the initial and final volume of the blastodiscs and yolk spheres were difficult to determine at exactly the same developmental stage. It may be argued that measurements could be initiated earlier, perhaps reducing the range of differences. However, deformation of the nascent zygote made it difficult to determine the blastodisc area at early developmental stages.

## Fast Movement of Ooplasm During the Early First Cleavage Division (Early Stage 1c)

### *Animal-Ward Movement of Endogenous and Exogenous Markers Along the Endoplasm.*

For this purpose, animations were prepared shortly before or by the time the actin ring started contracting. Phalloidin and actin immunostaining (n=12) showed that the referred ring formed by the accumulation of actin filaments at the margin of the blastodisc (not shown). Both the structure and contraction of the actin ring, associated with the arrival of a slow $Ca^{2+}$ wave from the animal pole, have been well documented by Leung et al. (1998, 2000). The contraction phase of the actin ring was accompanied by fast movement of animal and some vegetal endoplasmic inclusions, as well as yolk globules to the blastodisc (Fig. 6A,B; n=35). While inclusions moved along the interior of the axial and meridional streamers, large yolk globules did so along their surface. Tracking of fluorescent beads (n=20), microinjected in different regions of the yolk cell, made it possible to determine the existence of secondary pathways for endoplasm movement. The pattern of fast movement of inclusions and beads was similar in that, during the early first cleavage division, those

present in the streamers and lacunae at the animal hemisphere and upper sectors of the vegetal hemisphere moved first to the blastodisc (Fig. 6C–E). These results confirmed the orderly displacement of the endoplasm during the fast phase of movement. In the case of the meridional streamers, they transported inclusions and exogenous markers coming from peripheral lacunae, the interstice between the yolk globules or the neighbor ectoplasm. In the latter case, there were transient connections (Fig. 6F,G; see Supp. Video S6). During early stage 1c, inclusions in the axial streamers and emptying vegetal lacunae moved toward the blastodisc at high speeds (average 9.6 μm/min) following straight trajectories (Fig. 6H). Fluorescent beads moved similarly (Fig. 6I) but faster (average speed 39 μm/min). Inclusions and fluorescent beads in the meridional streamers moved to the blastodisc even faster, reaching an average speed of 40 and 73 μm/min, respectively. Meridional streamers thus constitute ultra-fast pathways for the animal-ward transport of the endoplasm. For statistical representation of the collected data, see Figure 6J and K. Differences in the speed of transport of inclusions and fluorescent beads across the cytoplasm have not yet been explained but may be related to the different mechanisms involved in their transport (see Beckerle, 1984).

Taking together the results of endoplasm movement during the slow and fast transport phases, we conclude that most of the animal endoplasm and part of the vegetal endoplasm are incorporated into the blastodisc during the first cell cycle.

### *Animal-Ward Movement of Endogenous and Exogenous Markers Along the Ectoplasm (n=7).*

During early stage 1c, inclusions and fluorescent beads in the animal ectoplasm and upper sectors of the vegetal ectoplasm preferentially moved toward the blastodisc at low (average 5.0 μm/min) or high (average 9.1 μm/min) speeds, respectively. Movement of inclusions in the rest of the vegetal ectoplasm exhibited great variations from zygote to zygote: they moved toward the vegetal pole, back and forth in different directions, or remained stationary (Fig. 7A–D). Hence, a steady flow of ectoplasm from vegetal to animal has not been visualized.

## Slow Movement of Ooplasm During the Late First Cleavage Division (Late Stage 1c, n=11)

Relaxation of the actin ring was accompanied by reverse movement (vegetal-ward) of animal ecto- and endoplasmic inclusions, including those that were already incorporated into the blastodisc. Yolk globules that invaded the blastodisc during the fast movement also returned to the yolk cell (Fig. 8A). The movement of these objects was slow (average speeds of 5.0 μm/min). Meanwhile, inclusions in the vegetal ecto and endoplasm moved in different directions or remained stationary.

## Movement of Endoplasm in the Parthenogenetic Egg and During Cleavage

Slow and fast movements of the ecto- and endoplasm, contraction/relaxation of the actin ring, formation of streamers and pseudo-cleavage took place in the unfertilized egg (n=25). These findings confirmed and complemented the observation of other investigators concerning with the properties of the activated non-fertilized egg (Kane and Kimmel, 1993; Webb et al., 1997).

The contraction/relaxation cycle of the actin ring also continued during cleavage (n=22) (see Kane and Kimmel, 1993) with inclusions and yolk globules slowly returning to the yolk cell during the relaxation phase and rapidly entering the blastodisc during the contraction phase (Fig. 8B,C). The speed of these movements was not determined. After a number of cleavage divisions, endoplasm was no longer visible in the yolk cell and large yolk globules in the blastodisc. By this time, separation of discernible yolk and ooplasm may be considered to have been completed. Gradually, thinner axial and meridional streamers formed during successive cycles of contraction/relaxation. Movement of inclusions across the ectoplasm of the cleaving embryo was not determined and, hence, it is not known whether its animal and vegetal sectors became functionally connected.

## Pulsations Are Blocked by Actin Toxins

Tracking of cytoplasmic inclusions (n=12), labeled beads, or dextran (n=8) by time-lapse video microscopy showed that during pulsations endoplasm moved back and forth along the animal/vegetal axis. Accordingly, animal-most endoplasm entered and exited the blastodisc after each pulsation. During low-frequency pulsations, endoplasmic inclusions moved slowly back and forth (average speed 5.0 μm/min), whereas during high-frequency pulsations they traveled back and forth faster (average speed 9.1 μm/min). Both types of pulsations were observed during the slow and fast phase of endoplasmic movements. The shortening and lengthening phase of each pulsation could take similar or different times. Hence, if the shortening phase of the pulsation was longer than the lengthening phase, more endoplasm entered than exited the blastodisc, and vice versa (Fig. 9A). Thus, pulsations may or may not contribute visible endoplasmic components to the blastodisc growth. In some cases, as that illustrated by the zygote of Supp. Video S5, generation of high-frequency pulsations was accompanied by changes in the direction of ooplasm movement. High-frequency pulsations could be asymmetric in that the two meridional halves of the zygote or embryo stretched and shortened out of phase. Accordingly, while endoplasm moved toward the animal pole in one half of the embryo, it moved away from the animal pole in the other half. This provoked marked deformations of the zygote or embryo. Pulsations are actin-dependent deformations because they were blocked after incubation in Cytochalasin B or Latrunculin B, but not in microtubule inhibitors such as

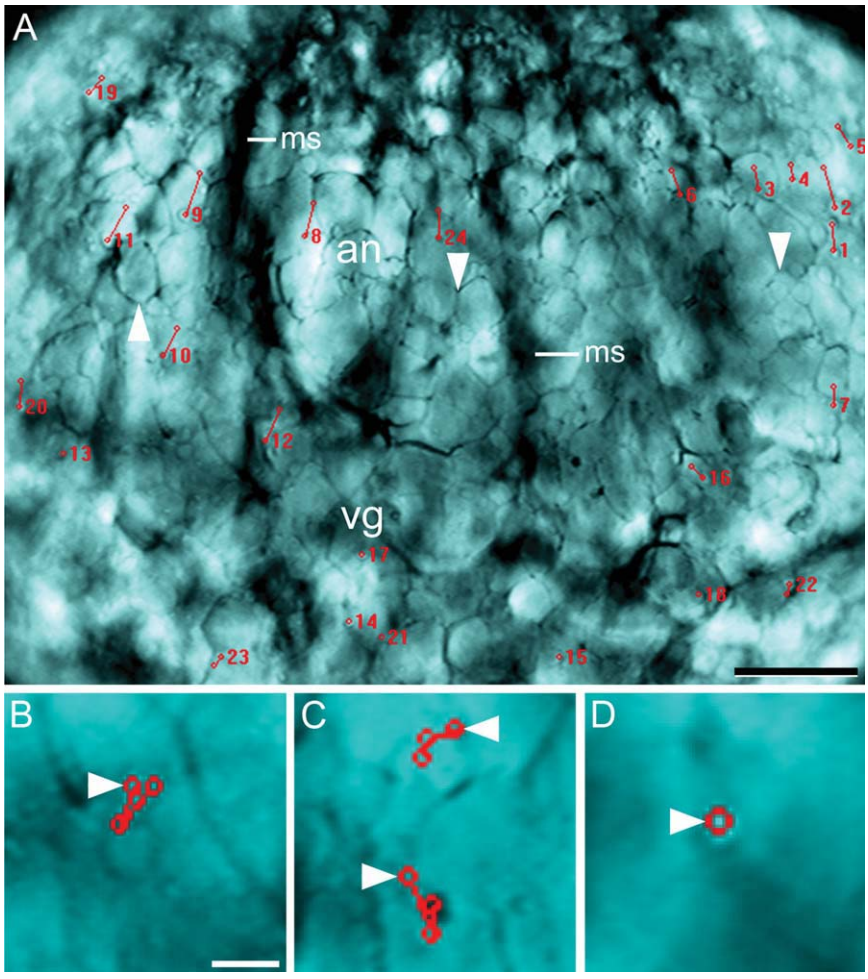


**Fig. 7.** Lateral view of a whole-mounted early stage 1c zygote that shows the movement of ectoplasmic inclusions. **A:** First image of a stack of 18 images, taken at intervals of 10 sec, showing the movement of inclusions across the animal (an) and vegetal (vg) ectoplasm. Numbers indicate the position of the inclusions at the time they initiated a run, which was marked with a straight line between the red circles. The outline of the peripheral yolk globules (arrowheads) and the silhouette of the meridional streamers (ms) are indicated. **B–D:** Higher magnification of regions of the same figure showing the behavior of inclusions in the vegetal ectoplasm: (B) back-and-forth movements, (C) change of direction, (D) lack of movement. The starting point is marked by an arrowhead. Scale bars = 80 μm (A), 15 μm (B–D).

Colchicine or Colcemide. As shown in Figure 9B and C, Cytochalasin B- and Latrunculin B-incubated zygotes (n=22) became flattened. They neither formed streamers nor contracted the actin ring (see also Leung et al., 2000), the blastodisc was smaller, and some endoplasmic lacunae became much larger than in the controls (Fig. 9D). Acid-fixed zygotes (n=25) also showed that the yolk cell contained fewer and larger endoplasmic lacunae that appeared greatly disconnected from one another (Fig. 9E). Acid-fixed controls incubated in 2% DMSO for the same time developed normally (Fig. 9F). Immunofluorescence staining for F-actin (n=18) in drug-treated zygotes showed that the actin network of endoplasmic lacunae (Fig. 9G,H) and that of the ectoplasm (Fig. 9J,K) broke into numerous rounded or irregularly shaped fluorescent aggregates, 1–5 μm in diameter, considered to be fragments of the actin network. Immunofluorescence staining of controls incubated in 2% DMSO revealed that the actin network in the endoplasm (Fig. 9I) and ectoplasm (Fig. 9L) remained unchanged. Actin fragments are considered equivalent to those described by Katow (1983) in Cytochalasin B–treated zebrafish eggs studied under the transmission electron microscope. Hence, the drugs provoked a severe disorganization of both the ectoplasmic (peripheral) and endoplasmic (internal) actin cytoskeletons. From these results, we conclude that the internal actin filaments may play a role in the generation of pulsations and contribute to maintain the organization of the endoplasmic lacunae.

## Maternal mRNAs Were Present in Endoplasmic Lacunae and Streamers

To ascertain the distribution of maternal gene products, in respect to different ooplasmic pathways, as well as the manner in which they could be transported to the blastodisc, whole-mount in situ hybridization was performed on the following mRNAs: *gsc, sqt*, and *vas*. The first two messengers move across the interior of the zygote (Bally-Cuif et al., 1998; Howley and Ho, 2000; Gore and Sampath, 2002), whereas *vas* moves along the periphery of the cell (Howley and Ho, 2000; Knaut et al., 2000). *In situ* hybridization of these messengers provided signals of different intensity. Strong signals are considered to suggest high concentration of the transcript, whereas weak signals indicate absence or lesser accumulation of the transcript.

### *Distribution of* gsc *and* sqt.

In the early first interphase zygote, *gsc* (n=42) and *sqt* (n=60) transcripts were present in the blastodisc, short streamers, and animal and vegetal endoplasmic lacunae (Fig. 10A,D), while at the beginning of the first cleavage division they were seen along the axial streamers (Fig. 10B, E). Hence, *gsc* and *sqt* transcripts probably reached the blastodisc along short and long axial streamers using slow and fast mechanisms of animal-ward transport. In the 2-cell embryo, *sqt* but not *gsc* transcripts were seen in the second-generation axial streamers (Fig. 10C,F). Differences in the distribution of these two mRNAs at similar periods of the

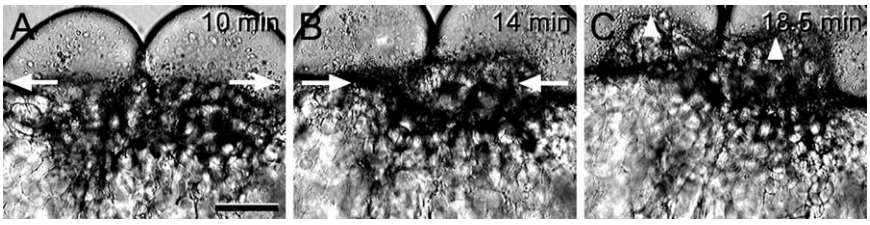


**Fig. 8.** Still frames from the time-lapse video animation of Figure 6A and B, taken at 10-sec intervals. **A:** Relaxation of the actin ring after formation of the 2-cell embryo. **B:** Contraction of the actin ring during the second cleavage division. **C:** Entry of endoplasm and yolk globules (arrowheads) into the two blastomeres. Time elapsed between the images is indicated. Development at 25°C. Scale bar = 115 μm (A–C).

second cell cycle suggest that *gsc* tends to move toward the animal pole during the first cell cycle, while *sqt* transcripts are still moving to the blastodisc during the second cell cycle. This may depend on factors such as amount of transcript available for transport in the zygote and/or the relative speeds at which transcripts moved.

### *Distribution of* vas.

In the first interphase zygote (Fig. 10G), *vas* (n=48) was found along the ectoplasm and blastodisc, while in the first cleavage division (Fig. 10H,I) it also appeared along the meridional streamers. Three conclusions may be drawn from these results. First, that *vas* moved animal-ward and accumulated at the blastodisc during the first interphase using the ectoplasmic pathway (see Theusch et al., 2006). Second, that during the first cleavage division meridional streamers may represent additional pathways for the animal-ward peripheral transport of the transcript. This conclusion is supported by the work of Howley and Ho (2000; see their fig. 3F) who visualized streaming lines (likely to be meridional streamers) of mRNA expression along the periphery of first cleavage embryos. Third, that discontinuity of the cytoplasmic flow between the vegetal and animal ectoplasms may have been solved by directing the animal-ward transport of vegetal *vas*, and perhaps of other transcripts, such as *dazl-like* (*dazl*) (Theusch et al., 2006), along the meridional streamers. In the 2-cell embryo (not shown), *vas* was present in the cleavage furrow (see also Pelegri et al., 1999).

## DISCUSSION

### Role of the Internal Cytoskeleton in the Orderly Animal-Ward Movement of Animal and Vegetal Endoplasm at Different Speeds

We have shown that endoplasm in different regions of the yolk cell reach the blastodisc along interconnected lacunae and streamers (see also Roosen-Runge, 1938; Lewis and Roosen-Runge, 1943; Hisaoka and Battle, 1958; Hisaoka and Firlit, 1960; Beams et al., 1985; Abraham et al., 1993; Leung et al., 2000). These structures are narrow spaces between the yolk globules, lack proper walls, and enclose numerous organelles (Hisaoka and Firlit, 1960; Katow, 1983: Fernández et al., 2006). In this report, we have shown that lacunae and streamers enclose a ubiquitous cytoskeleton of microtubules and actin filaments. This conclusion is supported by our previous work on transmission electron microscopy of zebrafish oocyte and eggs subjected to an improved fixation procedure using cytoskeleton stabilizers (Fernández et al., 2006). The use of stabilizers is needed because the endoplasmic cytoskeleton is delicate and hard to preserve. This probably explains why Katow (1983) failed to find microtubules and actin filaments in his electron microscope study of zebrafish axial streamers of routinely fixed zebrafish eggs. The fact that during different developmental periods ooplasmic inclusions and foreign markers move at different speeds and directions suggests the participation of various microtubule- and actin-based molecular motors. Since different transport pathways exhibit a similarly structured cytoskeleton, differences in speed may depend on the molecular motors available for transport at any given time. Our unpublished work, and that of Becker and Hart (1999), indicate that microtubule- and actin-based motors are present in the transport pathways, but their functional status is unknown. Information on this matter, and on the polarity of microtubules and actin filaments across different transport pathways, is needed. Animal/vegetal sequential emptying of endoplasmic lacunae by slow or fast streaming suggests that there may be an actin-based system of floodgates controlling the orderly mobilization of endoplasm. Fast animal-ward endoplasmic and slow vegetal-ward ectoplasmic streaming have been described in the zebrafish zygote by Leung et al. (2000). However, our findings on similar regions of the zygote at equivalent developmental periods show important differences. First, slow and fast streaming occurred both in the ecto- and endoplasm. Second, movement of the animal ectoplasm is preferentially directed toward the animal pole, whereas movement of the vegetal ectoplasm is multidirectional or negligible.

Differences in the speeds of movement reported by Leung et al (2000) may be explained by their use of higher temperatures compared to ours, and the fact that in the case of the endoplasm they tracked fluorescent beads instead of inclusions. We have shown that the beads move much faster. Slow and fast movement of ooplasmic inclusions have also been reported in the Medaka egg by Abraham et al. (1993). A better understanding of how microtubules and actin filaments engage in the slow and fast transport of different organelles and mRNA in live zygotes and early embryos requires the combined use of labeled organelles, tagged cytoskeletal components, and marked mRNAs.

### Fast Transport of Endoplasm Is Associated With Actin Contraction and Formation of Long Axial and Meridional Streamers

The zebrafish zygote and early embryo develop two pathways for the

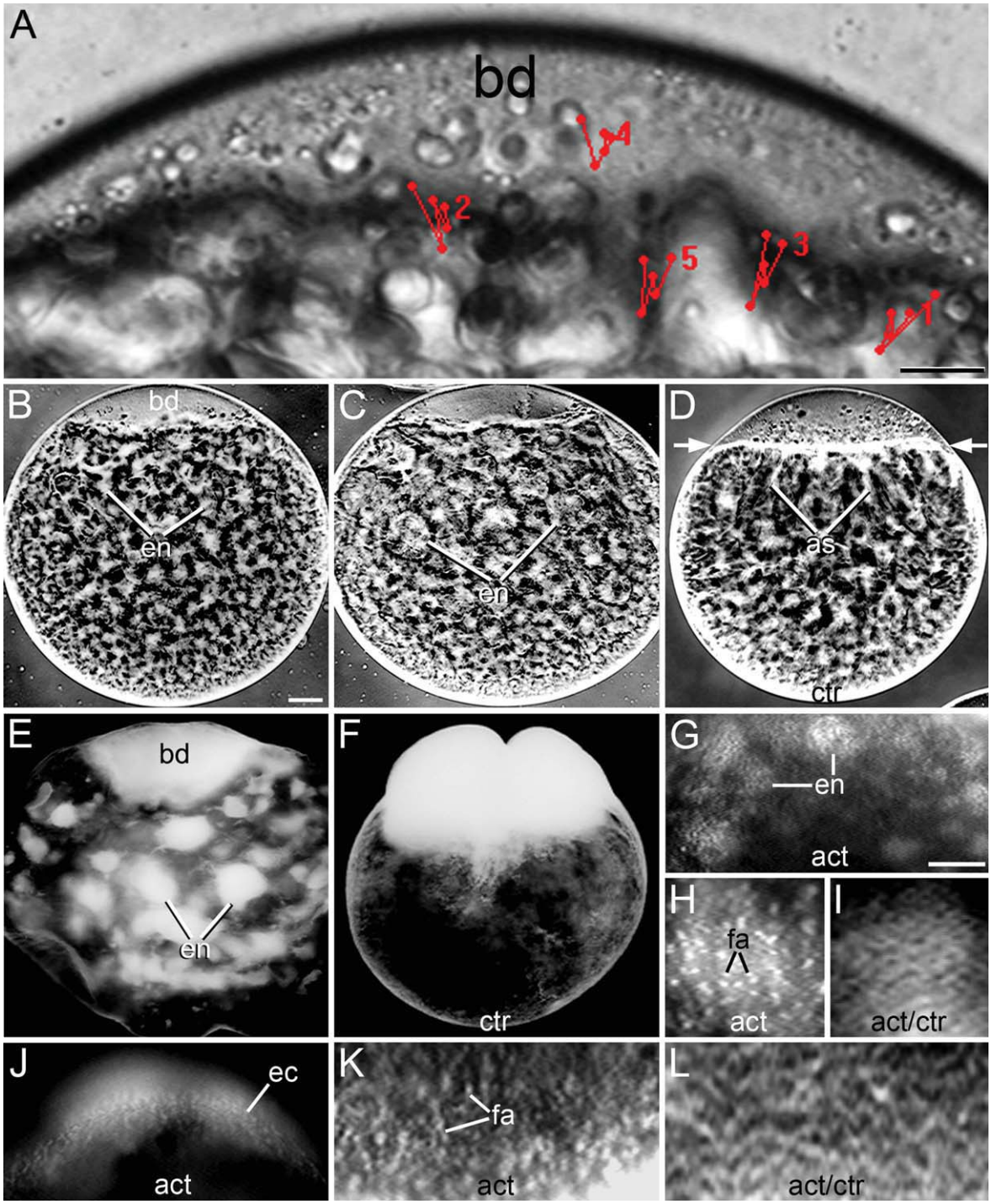


**Fig. 9.** Lateral view of whole-mounted zygotes showing the movement of inclusions during pulsations and the effect of actin poisons. **A:** Movement of 5 inclusions during a high-frequency pulsation in a stage 1b zygote. The time-lapse for each inclusion was taken independently at 10-sec intervals, marking the successive position of the inclusion with red dots and the path with straight lines linking the dots. Numbers indicate the initial position of the inclusion. The movement pattern of the inclusions was saved in the last image of the stack. Inverted contrast live (B–D) and acid-fixed (E, F) whole-mounted zygotes showing that blockade of pulsations after drug incubation was accompanied by disorganization of the endoplasmic lacunae. **B:** Incubation in Cytochalasin B for 45 min. **C:** Incubation in Latrunculin B for 2 hr. **D:** Control (ctr) incubated for 45 min in aquarium water with DMSO, showing that in this case the actin ring contracted and the axial streamers formed (as). **E:** Latrunculin B–treated zygote showing disruption and enlargement of the endoplasmic lacunae after 80-min incubation in the drug. **F:** Control zygote incubated for the same amount of time in 2% DMSO. Notice the absence of endoplasmic lacunae and the division of the blastodisc. **G,H:** Low- and high-magnification images of fragmented actin (fa) in endoplasmic lacunae of a zygote incubated in Cytochalasin B for 80 min. **I:** Actin network (act) in a lacuna of a control zygote incubated in 2% DMSO for the same amount of time. **J,K:** Low- and high-magnification images of fragmented actin in the ectoplasm (ec) of a zygote incubated in Latranculin B for 1 h. **L:** Actin network of a control zygote incubated for the same amount of time in 2% DMSO. Development at 25°C. bd, blastodisc. Scale bars = 16 μm (A), 60 μm (B–F), 45 μm (G ), 25 μm (H), 7 μm (I), 12 μm (J), 20 μm (K), 7 μm (L).

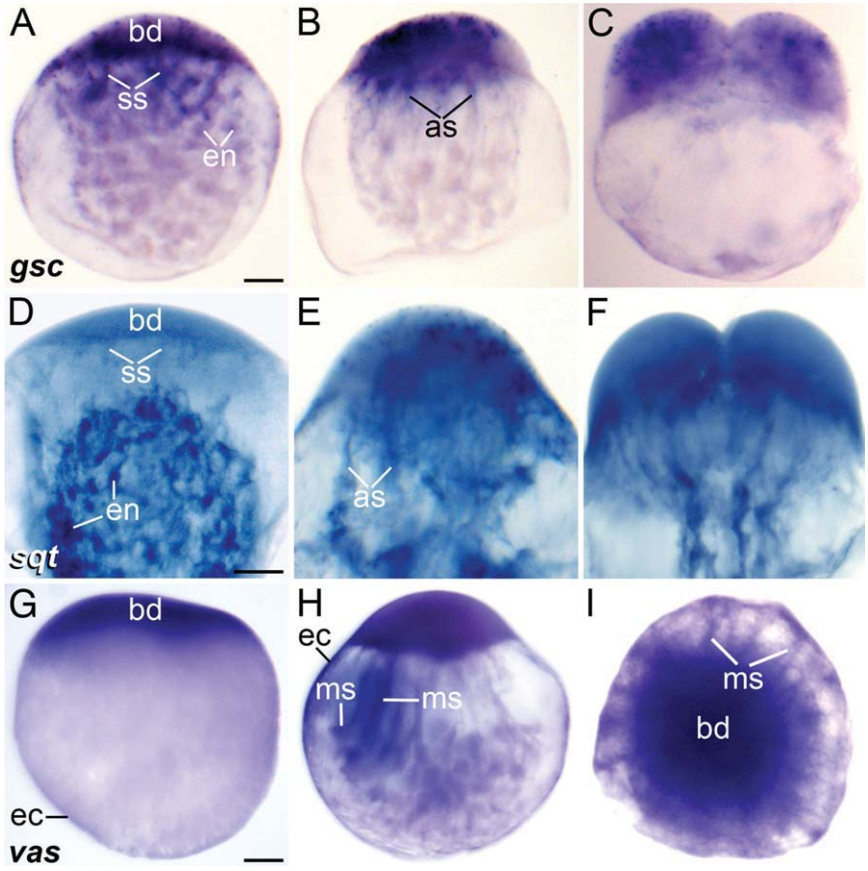


**Fig. 10.** Lateral (**A–H**) and animal pole (**I**) view of whole-mounted mid stage 1b zygotes (A, D, G), early stage 1c zygotes (B, E, H, I), and early two-cell embryos (C, F) showing the distribution of *gsc, sqt*, and *vas* mRNAs by in situ hybridization. The stage of development was determined by the size of the blastodisc, distribution of endoplasmic lacunae (when visible), contraction of the actin ring, and presence of streamers. Notice the distribution of the transcripts in different ooplasmic domains. Chromogenic substrate: BM purple (A–C and G–I) or NBT/BCIP (D–F). Scale bars = 90 μm (A–C, G–I), 70 μm (D–F).

fast transport of endoplasm: long axial and long meridional streamers. The long axial streamers were first described by Roosen-Runge (1938) in the zebrafish zygote, and later considered by other authors as the main pathway for endoplasmic movement (Leung et al., 2000). The long meridional streamers are described for the first time in this report. They constitute high-speed pathways for the transport of both endogenous and exogenous markers. According to data presented in this report, *vas* transcripts may also reach the blastodisc along the meridional streamers. Fluorescent beads in meridional streamers may reach speeds comparable to that of the fast axoplasmic flow (Grafstein and Forman, 1980).

Incubation of zygotes in Cytochalasin B (Katow, 1983; Leung et al., 2000) prevents contraction of the actin ring, formation of the long streamers, and blockade of the fast ooplasmic flow. Based on these results, Leung et al (2000) proposed that contraction of the cortical actin provides the power to drive the fast flow of endoplasm. However, our results indicate that Cytochalasin B and Latrunculin B also affect the integrity of the internal actin filaments, a situation that probably provokes interruption of streamer formation and blocks the flow of endoplasm. Hence, in addition to supporting the network of endoplasmic lacunae, internal actin filaments may also play an important role in ooplasmic flow. The signal that triggers contraction of the actin ring is associated with a rise of free cytosolic calcium, initiated at the sperm entry site and moving vegetal-ward peripherally, phenomenon that would presumably activate a myosin light chain kinase (Leung et al., 1998). A similar mechanism may be involved in the contraction of the internal actin cytoskeleton, a proposal that is supported by recent findings indicating that a wave of free calcium slowly moves vegetal-ward across the zygote central cytoplasm after activation (Sharma and Kinsey, 2008). Other evidence on the role of calcium in endoplasmic flow comes from the study of maternal-effect mutants such as *brom bones* (Mei et al., 2009). $IP_3$-mediated $Ca^{2+}$ release is impaired in the mutant, provoking alterations in the exocytosis of the cortical granules and cytoplasmic segregation. In conclusion, both peripheral and internal actin networks may participate in fast ooplasmic movements. Although movement of cortical (indeed ectoplasmic) fluorescent beads and dorsal determinants is claimed to depend on microtubules (Jesuthasan and Strähle, 1996), the overall function and properties of this cytoskeleton component in the zebrafish zygote are not fully understood.

## Animal, But Not Vegetal, Ectoplasm Appears to Move to the Blastodisc

Since one rarely finds animal and vegetal ectoplasmic inclusions moving in the same direction, the existence of a steady flow of ectoplasm from the animal to the vegetal pole, or vice versa, seems unlikely. This contradicts findings by Leung et al. (2000), who proposed the existence of an animal to vegetal flow of ectoplasm during the fast phase of ooplasmic segregation in the zebrafish zygote. According to these authors, the vegetally moving ectoplasm would return to the blastodisc via axial streamers, thus forming a counter-streaming system of ooplasmic flow. We have not found evidence of such an ooplasmic circuit. Instead, we have seen movement of fluorescent beads or ooplasmic inclusions from the endoplasmic lacunae to the animal ectoplasm or from the vegetal ectoplasm to the meridional streamers. In this report, we provide evidence that peripheral (sometimes called cortical) animally directed movement of fluorescent beads (see also Jesuthasan and Strähle, 1996), ooplasmic inclusions,

and maternal determinants, such as *vas* (Howley and Ho, 2000; Knaut et al., 2000; Pelegri, 2003), may occur along the meridional streamers.

Pole-ward movement of animal ectoplasm raises a question: how is animal ectoplasm replenished to provide continuous animal-ward movement during early and mid first interphase and early cleavage? One possibility is that components of the animal ectoplasm, such as organelles, are produced in situ by a replication machinery, as in leech eggs (Fernández et al., 1998). Alternatively, animal ectoplasm may be replenished by transfer of endoplasm from the neighbor yolk cell. The latter possibility is supported by results reported in this report and by Fernández et al. (2006). Interconnections between the ecto- and endoplasm would allow organelles and ribonucleoproteins to change pathways during their pole-ward journey. This matter is of importance for understanding how maternal transcripts and organelles reach the right place at the right time in the developing blastodisc or blastoderm. Intermittency of these interconnections suggests the existence of mechanisms regulating the flow of ooplasm between different speed pathways. It has been suggested that fluorescent beads moving along the ectoplasm end up in marginal blastomeres whereas those moving along the endoplasm are incorporated in central blastomeres (Jesuthasan and Strähle, 1996).

### Streamers Probably Constitute the Main Pathways for mRNAs to Reach the Blastodisc

Results on *gsc* distribution suggests that this transcript not only moves to the animal pole in the stage V oocyte (Bally-Cuif et al., 1998) but also moves animal-ward in the early zygote along short streamers and in the late zygote by means of long axial streamers. The distribution of *sqt* transcripts is similar and, hence, short and long axial streamers may also constitute their animal-ward transport pathways. Based on drug treatment, Gore and Sampath (2002) concluded that *sqt* transport is a microfilament-independent microtubule-dependent process. Since Latrunculin-treated zygotes do not form axial streamers and disrupt the endoplasm, *sqt* transcripts would move animal-ward by microtubules present along disorganized, probably less efficient, endoplasmic lacunae. This may explain why in Latrunculin-treated zygotes *sqt* accumulation in the blastodisc is reduced (Gore and Sampath, 2002). The distribution of *vas* suggests that this transcript moves animal-ward not only along the ectoplasm (Pelegri, 2003) but also by the meridional streamers. During slow transport, *vas* would move to the blastodisc along the ectoplasm. However, during fast transport our results suggest that localization of the transcripts along the ectoplasm and meridional streamers may be indicative that *vas* may be transported simultaneously along two different speed pathways. This may be also possible for other germ plasm components such as the *dazl* mRNA. This transcript has been reported to translocate toward the animal pole along the cortex (Theusch et al., 2006) during early embryogenesis (see also Kosaka et al., 2007), when meridional streamers still form. Meanwhile, other transcripts involved in germ plasm formation, such as *dnd* and *nos 1*, segregate during oogenesis and have already reached the blastodisc cortex in the freshly laid egg (Theusch et al., 2006). Animal-ward transportation of the *buc* mRNA also occurs during zebrafish oogenesis (Bontems et al., 2009). A better understanding of the routes for transcripts and protein translocation in the zygote and early embryo awaits further studies based on the tracking of labeled mRNA (Gore et al., 2005; Clark et al., 2007) and proteins (Bontems et al., 2009).

### Pulsations Are Striking Deformations of the Zygote and Early Embryo Whose Function Remains Unknown

Pulsations have not been reported before in the zebrafish zygote and early embryo. The great majority of the pulsations are fast and blocked by Cytochalasin B or Latrunculin B incubation, procedures that break the actin network in both the ecto- and endoplasm (see also Katow, 1983). Our results suggest that actin filaments participate in the generation of pulsations. The fact that pulsations may take place before one sees assembly of the actin ring, and the fact that this process also occurs during its relaxation phase, are taken as indicative that it is not the actin ring that participates in their occurrence and that it is the internal actin cytoskeleton that is involved. In addition, the appearance of asymmetric pulsations indicates that these may be generated by the alternate contraction of opposite sets of internal actin filaments, running along the endoplasmic lacunae and long streamers. Although pulsations constitute a striking phenomenon of cell deformation, their function in ooplasmic segregation is uncertain. It is possible that pulsations allow entry of very small non-detectable ooplasmic components, such as ribonucleoproteins, into the blastodisc or that they participate in their redistribution throughout the ooplasmic domains. In addition, pulsations may be involved in the closing or opening of the interconnections between lacunae or streamers and the ectoplasm. Pulsations may be triggered by weak calcium waves, some of which have been detected in the zebrafish endoplasm (Sharma and Kinsey, 2008).

## EXPERIMENTAL PROCEDURES

### Collection and Handling of Eggs and Zygotes

Adult zebrafish (*Danio rerio*) were maintained for a 14-hr light/10-hr dark photoperiod at 28°C in aquaria with circulating aerated water. Males and females were separated a day before and crossed the next day. To record developmental time, two females and one male were crossed at a time within the first 2 hr after the light turned on. Observations were performed at normal 28°C or lower 20–25°C. In the latter case, slower developmental rates allowed for studying quick events without affecting the normal progression of the cell cycle and the early events of ooplasmic segregation (see Fernández et al., 2006). Unfertilized eggs were obtained by

laparotomy of gravid mothers anesthetized with tricaine and activated in filtered aquarium water. About 1,000 eggs were used in this study.

## Preparation of Whole-Mounted Acid-Fixed Zygotes and Embryos

Mechanically dechorionated zygotes and early embryos were fixed in freshly prepared formaldehyde to which glacial acetic or iso-butyric acid (Merck pro analysis) were added. As a result of the acid fixation, the ooplasm became opaque while the yolk remained transparent. This result was much more pronounced with acetic than with iso-butyric acid. For eggs and early zygotes, 30–40 μl of acetic or 1 ml of iso-butyric acid was added to 3 ml of 5% freshly prepared formaldehyde. For late zygotes and embryos, 3–5 droplets of acetic or 5 droplets of isobutyric acid were added to the same amount of formaldehyde. Use of the invert contrast facility of the Metamorph program transformed the dark ooplasm into a whitish material and the transparent yolk into a dark background. Cells could be observed in the acid fixative or after 2 hr fixation followed by three 30-min rinses in 1× PBS. For more details, see Fernández et al. (2006).

## Drug Treatment

To determine the role of the cytoskeleton in the generation of pulsations, dechorionated early zygotes were incubated for 45 min, 80 min, or 2 hr in actin or microtubule poisons. In the first case, zygotes were incubated in Cytochalasin B (Sigma, St. Louis, MO) at a concentration of 0.02–0.03 mg/ml or in 0.1 mM Latrunculin B (Calbiochem, San Diego, CA), both diluted in aquarium water. In the second case, zygotes were incubated in Colchicine (Sigma) or Colcemide (Life Technologies, Norwalk, CT) at a concentration of 0.6 mg/ml in aquarium water. For the preparation of the stock solutions, the four drugs were diluted in DMSO (Sigma). Controls were incubated for the same amount of time in 0.75–2% DMSO in aquarium water. Drug-treated and control zygotes were studied in animations taken at 2-min intervals, after acid fixation or immunostaining for F-actin.

## Staining of Nuclear DNA With DAPI

Dechorionated zygotes were acid-fixed and their blastodiscs dissected out with fine scissors. After 2-hr fixation, the blastodiscs were rinsed in 3 changes of 1× PBS and then stained overnight at room temperature and continuous agitation in a 1 μg/ml solution of DAPI (Sigma) in 1× PBS. After 3× 1 hr rinse in 1× PBS, blastodiscs were mounted with glycerol/PBS between two cover slips separated by small plasticine stoppers. Samples were examined by combining DIC with fluorescence microscopy.

## Immunofluorescence Staining of Microtubules and Actin Filaments in Whole-Mounted and Frozen-Sectioned Zygotes

Zygotes at different stages of development were permeabilized for 30–45 min at room temperature in PHEM buffer (Schliwa, 1980; Schliwa and van Blerkom, 1981) containing 0.15% Triton X-100, anti-proteases, Taxol and Phalloidin (1 μg/ml) (all from Sigma). After 2-hr fixation in 4% freshly prepared paraformaldehyde or formaldehyde in 1× PBS, with the same concentration of Taxol and Phalloidin, zygotes were rinsed in several changes of 1× PBS for the same amount of time and blocked for 2 hr in 2% bovine serum albumin (BSA; Merck Research Laboratories, Rahway, NJ). For double staining of microtubules and actin filaments, zygotes were incubated in monoclonal IgG anti-α-tubulin (Calbiochem) and monoclonal IgM antiactin (Calbiochem) 1:100 in 1× PBS/Triton/BSA for 24 hr at room temperature. After several rinses in 1× PBS for 2–4 hr, zygotes were incubated in 1:100 Alexa Fluor 594 goat antimouse IgG (Molecular Probes, Eugene, OR) and 1:100 Cy2 goat antimouse IgM (Jackson, West Grove, PA) in 1× PBS/Triton/BSA for another 24 hr at room temperature. Antiactin was sometimes replaced by labeled Phalloidin (1 μg/ml; Molecular Probes). After rinsing in 1× PBS, zygotes were either whole-mounted between coverslips separated by plasticine stoppers or soaked in 30% sucrose until they reached the bottom of an Eppendorf tube. Then, 15–20-μm-thick frozen sections were mounted between coverslips. In both cases, 9:1 glycerol/PBS was used as mounting medium. Control zygotes were only incubated in the second antibody at a concentration of 1:100. We also prepared control zygotes microinjected with labeled dextran and examined them under the fluorescence microscope. For more details, see Fernández and Olea (1995). To determine whether microtubules of the endoplasmic cytoskeleton could be revealed by immunofluorescence methods used by others in the zebrafish embryo, zygotes were prepared according to Jesuthasan and Strähle (1996). To ensure that the antibodies would penetrate sufficiently into the zygote, cells were fragmented after fixation.

## In Situ Hybridization of Whole-Mounted Zygotes

In situ hybridization was performed in early stage-1b and -1c zygotes and two-cell embryos. The following transcripts were detected using the corresponding anti-sense mRNA: *squint* (*sqt*), *goosecoid* (*gsc*), and *vasa* (*vas*). They were prepared from plasmids kindly donated by L. Valdivia (*gsc*), V. Gallardo (*sqt*), and F. Pelegri (*vas*). The purified plasmidial DNAs were linearized with appropriate restriction enzymes and used as templates for the synthesis of the antisense mRNA using digoxigenin-bound nucleotides.

For hybridization, cells were first permeabilized-fixed as for immunofluorescence, rinsed in PBST (1× PBS + 0.1% Tween 20, Sigma) for 2 hr, digested with proteinase K (Roche, Nutley, NJ), postfixed, and rinsed again in PBST. Zygotes and embryos were then treated with hybridization buffer for 4 hr at 65°C, and hybridized overnight at 65°C in hybridization buffer containing 0.5–1 μg/ml of the marked synthetic antisense mRNA. After hybridization, zygotes were rinsed at the same temperature in decreasing concentrations of formamide (Carlo Erba, Milan, Italy) in sodium chloride/sodium citrate (SSC)

and finally in pure SSC. Cells were then blocked, incubated for 8 hr in anti-digoxigenin conjugated with alkaline phosphatase (Roche) 1:2,000, and rinsed in PBST. Released phosphate was revealed with a chromogenic substrate, either NBT/BCIP (Sigma) or BM Purple (Roche), rinsed in 1× PBS, and mounted in 9:1 glycerol 1× PBS. For more details see Thisse and Thisse (2008).

## Tracking of Cytoplasmic Inclusions, Microinjected Fluorescent Dextran, and Latex Beads

To trace cytoplasmic movements and determine the speed and direction at which ooplasm is transported across the zygote, the movement of cytoplasmic inclusions, 10-kDa fluorescent dextran, or 1 μm in diameter fluorescent beads (Molecular Probes) were used. The probes were dissolved in glutamate buffer (Hyman et al., 1991) to a final dextran concentration at the pipette of 25–50 mM, and 0.2%, for the beads. A total of 4 nl of each probe was microinjected in the yolk cell, an amount that represented less than 5% of the zygote volume (about 200 nl). A Narishige IM 300 microinjector was used. For more details, see Fernández et al. (2006). Zygotes were microinjected at early stage 1b. Labeled dextran rapidly diffused from the injection site and in a short time filled all the ooplasmic domains. For that reason, labeled dextran was microinjected at the center of the yolk cell. Labeled beads, on the contrary, filled lacunae at the injection site and moved with the ooplasm. Therefore, in this case microinjections had to be placed close to the region under study. Tracking of labeled probes was performed in time-lapse animations taken at 10–30-sec intervals. Objects were tracked until they became out of focus, marking their position at each time interval. The point track option of Metamorph traced a line along the successive time-point intervals recreating the path of the object. The software indicated the speed of the object during each time interval as well as its total speed during the run. Back-and-forth movements may be fast and tracking of the objects in this case was reduced to a minimal time interval of 5 sec.

## Video and Confocal Microscopy and Image Processing

Whole-mounted uninjected live, acid-fixed, immunostained, or microinjected zygotes and embryos were examined in a Zeiss 135 inverted light, DIC and fluorescence microscope equipped with a Z motor (Prior) and a Hamamatsu chilled CCD camera (model C5985). For lower magnification, Achroplan objectives (×10–40) were used. For higher magnification, a Plan Neofluar objective (×100, NA 1.4) and the Optovar (×1.6–2.5) allowed the projection of images onto the camera chip at 160–250 magnification. Image grabbing and processing were performed on a PC computer using the Metamorph 6.1 version. Immunostained whole-mounted zygotes were also examined in a confocal Zeiss LSM 510 META laser scanning microscope equipped with argon and He-Ne lasers; 20/0.5, 40/0.75, and 63/1.4 objectives were used. Optical sections every 1–2 μm allowed the preparation of Z-stacks utilized in the manufacture of projections and cuts in the x and y axes. Confocal images were deconvolved with the Huygens Professional software version 3.5.

## Statistical Analysis of Data on the Speed of Ooplasmic Inclusions

A total of 674 speed determinations (runs) of ooplasmic inclusions and 145 runs of fluorescent beads, moving preferentially to the animal pole, were collected from 30 zygotes developing at 23–25°C. A frequency histogram of the determined speeds was constructed using 2 μm per second bins. The distribution of the speeds was described in the form of Gaussian curves. Central values and standard deviations of the Gaussian functions were found using the Regression Wizard of Sigmaplot 10.0. With this information, three Gaussian curves representing slow, fast, and ultrafast speed-moving inclusions or fluorescent beads were prepared.

## Determination of the Blastodisc and Yolk Cell Volumes During the First Interphase

To quantify the slow animal-ward movement of ooplasm, changes in the volume of the blastodisc and yolk cell were determined in 10 live chorionated whole-mounted zygotes developing at 25°C. Zygotes with the animal/vegetal axis oriented parallel to the microscope stage were used. Each zygote was video-imaged twice: first 5–15 min after activation (early stage 1b) and then close to the initiation of the actin ring contraction (late stage 1b). Images acquired at 200× magnification in the screen were printed on squared paper at a final magnification of 230×. The blastodisc area was outlined and subdivided in 4- or 2-mm-wide ($w_i$) intervals, the height ($h_i$) and radius ($r_i$) of which were determined. The volume of the blastodisc (V) was finally calculated for each zygote at the two time points referred to above, using the formula $V = [2\pi/(230)^3] \Sigma_i (r_i\ h_i w_i)$. The volume of the yolk cell was calculated by the formula $4/3\ \pi r^3$. Since the yolk cell is not a perfect sphere, the final radius was determined as the average length of several radii drawn on the squared paper.

## ACKNOWLEDGMENTS

We thank Dr. O. Alvarez and U. Carrera for help on the statistical analysis of data, V. Guzmán, L. Ossa, L. Saragoni, F. Oyarzún, and O. Ramírez for technical assistance. L. Valdivia, V. Gallardo, and F. Pelegri for donation of plasmids, and Drs. C. Connelly and J. Nicholls for critical reading of the manuscript. We acknowledge the contribution of funds for the purchase of reagents and maintenance of the animal room from the University of Chile.

## REFERENCES

Abraham VC, Gupta S, Fluck RA. 1993. Ooplasmic segregation in the medaka *Oryzias latipes* egg. Biol Bull 184: 115–124.

Bally-Cuif L, Schatz WJ, Ho RK. 1998. Characterization of the zebrafish Orb/CPEB-related RNA-binding protein and localization of maternal components in the zebrafish oocyte. Mech Dev 77: 31–47.

Bashirullah A, Cooperstock RL, Lipshitz HD. 1998. RNA localization in development. Annu Rev Biochem 67:335–394.

Beams HW, Kessel RG, Shih CY, Tung HN. 1985. Scanning electron microscopy studies on blastodisc formation in the zebrafish, *Brachidanio rerio*. J Morphol 184:41–39.

Becker KA, Hart NH. 1996. The cortical actin cytoskeleton of unactivated eggs: spatial organization and distribution of filamentous actin, nonfilamentous actin and myosin-II. Mol Reprod Dev 43: 536–547.

Becker KA, Hart NH. 1999. Reorganization of filamentous actin and myosin II in zebrafish eggs correlates temporally and spatially with cortical granule exocytosis. J Cell Sci 112:97–110.

Beckerle MC. 1984. Microinjected fluorescent polysterene beads exhibit saltatory motion in tissue culture cells. J Cell Biol 98:2126–2132.

Bontems F, Stein A, Marlow F, Lyautey J, Gupta T, Mullins MC, Dosch R. 2009. Bucky ball organizes germ plasm assembly in zebrafish. Curr Biol 19:1–9.

Clark A, Meignin C, Davis I. 2007. A dynein-dependent shortcut rapidly delivers axis determination transcripts into the *Drosophila* oocyte. Development 134:1955–1965.

Conklin EG. 1905. The orientation and cell lineage of the ascidian egg. J Acad Nat Sci Phila 13:5–119.

Créton R, Speksnijder JE, Jaffe LF. 1998. Patterns of free calcium in zebrafish embryos. J Cell Sci 111:1613–1622.

Dekens MPS, Pelegri F, Maischein HM, Nüsslein-Volhard C. 2003. The maternal-effect gene *futile cycle* is essential for pronuclear congression and mitotic spindle assembly in the zebrafish zygote. Development 130:3907–3916.

Dosch R, Wagner DS, Mintzer KA, Runke G, Wiemelt AP, Mullins MC. 2004. Maternal control of vertebrate development before the mid-blastula transition: mutants from the zebrafish. Dev Cell 6: 771–780.

Fernández J, Olea N. 1982. Embryonic development of glossiphoniid leeches. In: Harrison FW, Cowden RR, editors. Developmental biology of freshwater invertebrates. New York: Alan R. Liss. p 317–361.

Fernández J, Olea N. 1995. Formation of the female pronucleus and reorganization and disassembly of the first interphase cytoskeleton in the egg of the glossiphoniid leech *Theromyzon rude*. Dev Biol 171:541–553.

Fernández J, Olea N, Ubilla A, Cantillana V. 1998. Formation of polar cytoplasmic domains (teloplasms) in the leech egg is a three-step segregation process. Int J Dev Biol 42:149–162.

Fernández J, Valladares M, Fuentes R, Ubilla A. 2006. Reorganization of cytoplasm in the zebrafish oocyte and egg during early steps of ooplasmic segregation. Dev Dyn 235:656–671.

Gore AV, Sampath K. 2002. Localization of transcripts of the zebrafish morphogen *squint* is dependent on egg activation and the microtubule cytoskeleton. Mech Dev 112:153–156.

Gore AV, Maegawa S, Sheong A, Gilligan PC, Weinberg ES, Sampath K. 2005. The zebrafish dorsal axis is apparent at the four-cell stage. Nature 438: 1030–1035.

Grafstein B, Forman DS. 1980. Intracellular transport in neurons. Physiol Rev 60:1167–1283.

Hart NH, Fluck RA. 1995. Cytoskeleton in teleost eggs and early embryos: contributions to cytoarchitecture and motile events. In: Capco ED, editor. Current topics in developmental biology. Orlando, FL: Academic Press. p. 343–381.

Hart NH, Becker KA, Wollenski JS. 1992. The sperm entry site during fertilization of the zebrafish egg: localization of actin. Mol Reprod Dev 32:217–228.

Hashimoto Y, Maegawa S, Nagai T, Yamaha E, Suzuki H, Yasuda K, Inoue K. 2004. Localized maternal factors are required for zebrafish germ cell formation. Dev Biol 268:152–161.

Hisaoka KK, Battle HI. 1958. The normal developmental stages of the zebrafish *Brachidanio rerio* (Hamilton-Buchanan). J Morphol 102:311–328.

Hisaoka KK, Firlit CF. 1960. Further studies on the embryonic development of the zebrafish, *Brachidanio rerio* (Hamilton-Buchanan). J Morphol 197:205–255.

Howley C, Ho RK. 2000. mRNA localization patterns in zebrafish oocytes. Mech Dev 92:305–309.

Hyman E, Drechsel D, Kellogg D, Salser S, Sawin K, Steffen P, Wordeman L, Mitchison T. 1991. Preparation of modified tubulins. Methods Enzymol 196: 478–485.

Ivanenkov VV, Meshcheryakov VN, Martynova LE. 1990. Surface polarization in loach eggs and two-cell embryos: correlations between surface relief, endocytosis and cortex contractility. Int J Dev Biol 34:337–349.

Iwamatzu T. 1973. On the mechanisms of ooplasmic segregation upon fertilization in *Oryzias latipes*. Jpn J Ichtyo 20: 73–78.

Jeffery WR, Meier S. 1983. A yellow crescent cytoskeletal domain in ascidian eggs and its role in early development. Dev Biol 96:125–143.

Jesuthasan S, Strähle U. 1996. Dynamic microtubules and specification of the zebrafish embryonic axis. Curr Biol 7: 31–42.

Kane DA, Kimmel CB. 1993. The zebrafish midblastula transition. Development 119:447–456.

Katow H. 1983. Obstruction of blastodisc formation by cytochalasin B in the zebrafish, *Brachidanio rerio*. Dev Growth Differ 25:477–484.

Kishimoto Y, Koshida S, Furutani-Seiki M, Kondoh H. 2004. Zebrafish maternal-effect mutations causing cytokinesis defect without affecting mitosis or equatorial vasa deposition. Mech Dev 121: 79–89.

Knaut H, Pelegri F, Bohmann K, Schwarz H, Nüsslein-Volhard C. 2000. Zebrafish vasa RNA not its protein is a component of the germ plasm and segregates asymmetrically before germline specification. J Cell Biol 149:875–888.

Kosaka K, Kawakami K, Sakamoto H, Inoue K. 2007. Spatiotemporal localization of germ plasm RNAs during zebrafish oogenesis. Mech Dev 124:279–289.

Lee KW, Webb SE, Miller AL. 2006. Requirement for a localized $IP_3$ R-generated $Ca^{2+}$ transient during the furrow positioning process in zebrafish zygotes. Zygote 14:143–155.

Lessman CA. 2009. Oocyte maturation. Converting the zebrafish oocyte to the fertilizable egg. Gen Comp Endocrinol 161:53–57.

Leung CF, Webb SE, Miller AL. 1998. Calcium transients accompany ooplasmic segregation in zebrafish embryos. Dev Growth Differ 40:313–326.

Leung CF, Webb SE, Miller AL. 2000. On the mechanism of ooplasmic segregation in single-cell zebrafish embryos. Dev Growth Differ 42:29–40.

Lewis WH, Roosen-Runge EC. 1943. The formation of the blastodisc in the egg of the zebrafish, *Brachidanio rerio*. Anat Rec 85:326.

Lillie RS. 1906. Observations and experiments concerning the elementary phenomena of embryonic development in *Chaetopterus*. J Exp Zool 3:153–268.

Lindeman RE, Pelegri F. 2009. Vertebrate maternal-effect genes: Insights into fertilization, early cleavage and germ cell determinant localization from studies in the zebrafish. Mol Reprod Dev 77: 299–313.

Mahowald AP. 1962. Finer structure of pole cells and polar granules in *Drosophila melanogaster*. J Exp Zool 228: 91–-97.

Marlow FL, Mullins MC. 2008. Bucky ball functions in Balbiani body assembly and animal-vegetal polarity in the oocyte and follicle cell layer in zebrafish. Dev Biol 321:40–50.

Mei WM, Lee KW, Marlow FL, Miller AL, Mullins MC. 2009. hnRNP I is required to generate the $Ca^{2+}$ signal that causes egg activation in zebrafish. Development 136:3007–3017.

Mizuno T, Yamaha E, Kuroiwa A, Takeda H. 1999. Removal of vegetal yolk causes dorsal deficiencies and impairs dorsal-inducing ability of the yolk cell in zebrafish. Mech Dev 81:51–63.

Nelsen OE. 1953. Comparative embryology of the vertebrates. New York: Blakiston Co. 982 p.

Ober EA, Schulte-Merker S. 1999. Signals from the yolk cell induce mesoderm, neuroectoderm, the trunk organizer and the notochord in zebrafish. Dev Biol 215:167–181.

Pelegri F. 2003. Maternal factors in zebrafish. Dev Dyn 228:535–554.

Pelegri F, Knaut H, Maischein HM, Schulte-Merker S, Nüsslein-Volhard C. 1999. A mutation in the zebrafish maternal-effect gene *nebel* affects

furrow formation and *vasa* RNA localization. Curr Biol 9:1431–1440.

Penners A. 1922. Die furchung von *Tubifex rivulorum*. Lam Zool Jb Abt Anat Ontog 43:323–367.

Roosen-Runge EC. 1938. On the early development-bipolar differentiation and cleavage of the zebrafish, *Brachidanio rerio*. Biol Bull 75:119–133.

Schliwa M. 1980. Structural organization of detergent-extracted cells. In: Bailey GW, editor. Proceedings of the 38th Meeting of Electron Microscopy Society of America. Baton Rouge, LA: Claitors. p. 814–817.

Schliwa M, van Blerkom J. 1981. Structural interactions of cytoskeletal components. J Cell Biol 90:222–235.

Sharma D, Kinsey WH. 2008. Regionalized calcium signaling in zebrafish fertilization. Int J Dev Biol 52:561–570.

Shimizu T. 1982. Development in the freshwater oligochaete *Tubifex*. In: Harrison FW, Cowden RR, editors. Developmental biology of freshwater invertebrates. New York: Alan R. Liss. p. 283–316.

Streisinger G, Walker C, Dower N, Knauber G, Singer F. 1981. Production of clones of homozygous diploid zebrafish (*Brachidanio rerio*). Nature 291:293–296.

Strome S, Wood WB. 1983. Generation of asymmetry and segregation of germ-like granules in early *Caenorhabditis elegans* embryos. Cell 35:15–25.

Theusch EV, Brown KJ, Pelegri F. 2006. Separate pathways of RNA recruitment lead to the compartmentalization of the zebrafish germ plasm. Dev Biol 292: 129–141.

Thisse C, Thisse B. 2008. High-resolution in situ hybridization to whole-mount zebrafish embryos. Nature Protocols 3: 59–69.

Urven LE, Yabe T, Pelegri F. 2006. A role for non-muscle myosin II function in furrow maturation in the early zebrafish embryo. J Cell Sci 119:4342–4352.

Webb SE, Lee KW, Karplus E, Miller AL. 1997. Localized calcium transients accompany furrow positioning, propagation, and deepening during the early cleavage period of zebrafish embryos. Dev Biol 192:78–92.

Whitman CO. 1878. The embryology of Clepsine. J Microsc Sci 18:215–315.

Wilson EB. 1904. Experimental studies on germinal localization. I. The germ regions of the egg of *Dentalium*. II. Experiments on the cleavage-mosaic in *Patella* and *Dentalium*. J Exp Zool 1:1–72.

Developmental Dynamics